Two Nonmuscle Myosin II Heavy Chain Isoforms Expressed in Rabbit Brains: Filament Forming Properties, the Effects of Phosphorylation by Protein Kinase C and Casein Kinase II, and Location of the Phosphorylation Sites†

Noriko Murakami,* Ved P. S. Chauhan, and Marshall Elzinga*

Institute for Basic Research in Developmental Disabilities, 1050 Forest Hill Road, Staten Island, New York 10314

Received August 8, 1997; Revised Manuscript Received November 3, 1997

ABSTRACT: During the course of the expression of a 47-kDa COOH-terminal fragment of brain-type nonmuscle myosin heavy chain (MIIB^{F47}), we found two closely related forms of MIIB, designated MIIB$^{\alpha}$ and MIIB$^{\beta}$, in rabbit brains. The B$^{\alpha}$ form corresponded to SM_{emb}, described by Kuro-o et al. [(1991) *J. Biol. Chem. 266*, 3768] and was the more abundant form in rabbit brain, while the B$^{\beta}$ form was novel. MIIB$^{\beta F47}$ differed from MIIB$^{\alpha F47}$ at six positions, three of which were within the carboxyl-terminal nonhelical domain; in MIIB$^{\beta F47}$, Ser, Pro, and Lys replaced Pro, Ser, and Glu, respectively. MIIB$^{\alpha F47}$ and MIIB$^{\beta F47}$ differed in filament assembly properties in the presence of various concentrations of salt, and a chimera containing the helical domain of MIIB$^{\beta F47}$ and the nonhelical domain of MIIB$^{\alpha F47}$ behaved very much like MIIB$^{\beta F47}$. Protein kinase C (PK C) incorporated 1 and 2 mol of phosphate/mol peptide of MIIB$^{\alpha F47}$ and MIIB$^{\beta F47}$, respectively, and caused similar levels of inhibition of assembly for both isoforms. Casein kinase II (CK II) incorporated 4 and 2 mol of phosphate/mol of MIIB$^{\alpha F47}$ and MIIB$^{\beta F47}$ peptides, respectively, and this caused strong inhibition of assembly for MIIB$^{\alpha F47}$ but only slight inhibition for MIIB$^{\beta F47}$. PK C sites in MIIB$^{\alpha F47}$ were localized within a region containing a cluster of Ser residues near the predicted junction of the helical and nonhelical domains: P-I-S(PO_4)-F-S(PO_4)-S(PO_4)-S(PO_4)-R-S(PO_4)-. Out of the five potential PK C sites, only one site seemed to be phosphorylated per peptide. The PK C sites in MIIB$^{\beta F47}$ were localized as S(PO_4)-I-S-F-S-S-(PO_4)-R-S(PO_4)-, with total incorporation of about 2 mol/mol of peptide. In addition, PK C phosphorylated a Ser within the predicted helical domain, E-V-S(PO_4)-T-L, in both MIIB$^{\alpha F47}$ and MIIB$^{\beta F47}$. For CK II, five sites were identified within the COOH end of MIIB$^{\alpha F47}$: S(PO_4)-L-E-L-S(PO_4)-D-D-D-T(PO_4)-E-S-K-T-S(PO_4)-D-V-N-E-T-Q-P-P-Q-S(PO_4)-E. The same sites were phosphorylated in MIIB$^{\beta F47}$ except for the first Ser, which was replaced by Pro in MIIB$^{\beta F47}$. An average of about two of the four potential sites were phosphorylated in MIIB$^{\beta F47}$, while in MIIB$^{\alpha F47}$ all five sites could be fully phosphorylated by CK II. Our results demonstrate that (1) the helical domains dictate the intrinsic salt dependence of assembly for nonmuscle myosin, (2) the isoforms are phosphorylatable by different kinases in an isoform specific manner mostly within the COOH-terminal nonhelical domain, and (3) the effects of the phosphorylation on assembly are isoform specific.

Myosins are molecular motors expressed in both muscle and nonmuscle cells. Conventional myosins (myosin II) found in cytoplasm are called "nonmuscle" or "cellular" myosins and participate in cell motility in conjunction with filamentous actin. In contrast to the muscle myosins which form stable myofibrils, nonmuscle myosins exhibit a dynamic monomer ↔ filament equilibrium that shifts according to changes in cellular functions and motilities (*1*). Higher vertebrates have at least two genes for nonmuscle myosin II, MIIA[1] (macrophage type) and MIIB (brain type) (*2*−*4*), and filaments of these myosins have been shown to distribute within cells in isoform-specific patterns (*5*−*8*). This suggests that cells have mechanism(s) to regulate myosin assembly in an isoform-specific manner.

Various vertebrate nonmuscle and smooth muscle myosin isoforms have been sequenced (*2*−*4*, *9*−*16*). Both nonmuscle and smooth muscle myosins contain a carboxyl-terminal tail piece (nonhelical domain) not found in striated muscle myosins. Sequence comparisons reveal that the helical coiled-coil domains of MIIA, MIIB, and smooth muscle myosin heavy chains are quite well conserved. In contrast, the sequences of the COOH-terminal nonhelical tail domains are isoform specific and are highly conserved across species lines (see Figure 1). It is well accepted that, in vertebrates, filament formation of smooth muscle and nonmuscle myosins is regulated by phosphorylation of the light chains. However, the nonhelical domains too are known to

† This work was supported by the New York State Office of Mental Retardation and Developmental Disabilities.

* Corresponding authors: phone, 718-494-5324; fax, 718-698-7916; e-mail, PJISADOG@interport.com (N.M.) or NCXM46A@prodigy.com (M.E.).

[1] Abbreviations: MIIA^{F46}, COOH-terminal 46-kDa fragment of macrophage-type myosin heavy chain; MIIB$^{\alpha F47}$ and MIIB$^{\beta F47}$, COOH-terminal 47-kDa fragments of rabbit brain type myosin heavy chain isoforms of α and *β*; PS, phosphatidylserine; PK C, protein kinase C; CK II casein kinase II; PTH, phenylthiohydantoin; HPLC, high-performance liquid chromatography; TFA, trifluoroacetic acid.

S0006-2960(97)01959-4 CCC: $15.00
Published on Web 01/30/1998

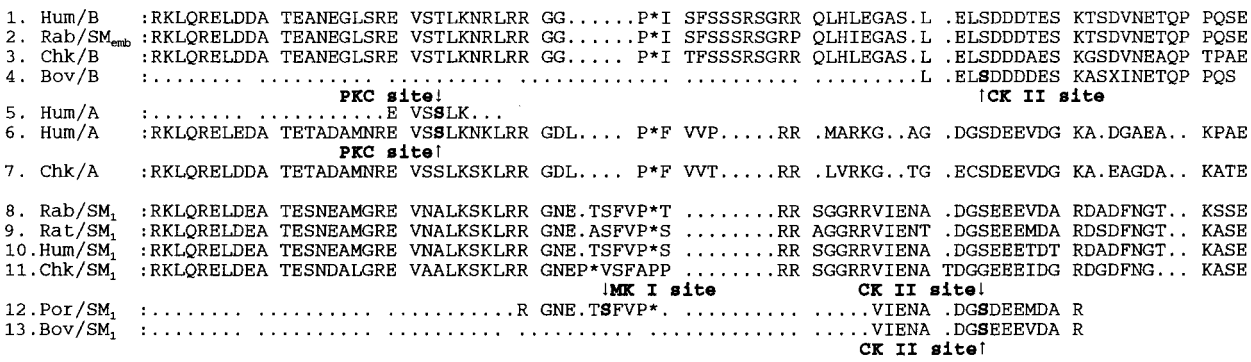

FIGURE 1: Amino acid sequences of the COOH-terminal regions of nonmuscle and smooth muscle myosin heavy chain isoforms. Amino acid sequences of myosin heavy chains from (1) human B (*12*), (2) rabbit MIIB (SM_{emb}) (*11*), (3) chicken brain (*10*), (4) bovine brain (*23*), (5) human platelet (*25*), (6) human macrophage (*2*), (7) chicken intestinal epithelium (*9*), (8) rabbit uterus SM_1 (*14*), (9) rat aorta SM_1 (*13*), (10) human smooth muscle SM_1 (*16*), (11) chicken gizzard (15), (12) porcine aortic SM_1 (*40*), and (13) bovine aortic SM_1 (*24*). An asterisk (*) is the Pro marking the beginning of the nonhelical tail domain. CK II, PK C sites, and MK I (myosin heavy chain kinase I; *40*) (bold Ser) that have been previously reported are shown by arrows.

influence assembly of myosins in vitro (*17*−*21*) and in vivo (*22*). They contain sites for phosphorylation by casein kinase II (CK II) in vitro and in vivo (*23, 24*). Protein kinase C (PK C) was shown to phosphorylate a single site near the end of the α-helical domain of human platelet myosin and MIIA both in vitro and in vivo (*25, 26*). On the basis of these observations, we hypothesize that, in addition to the light chain-mediated regulation of assembly, phosphorylation of heavy chains within their nonhelical domain also regulates nonmuscle myosins II assembly and that the effects of the heavy chain phosphorylation are isoform specific. To test our hypothesis, we have been using fragments from the COOH-terminals of myosin heavy chains expressed in *Escherichia coli*, as a model system. Phosphorylation by PK C affected assembly of heavy chain fragments of the rabbit brain-type myosin (405 amino acid residues, $MIIB^{F47}$) but not that of human macrophage myosin (396 amino acid residues, $MIIA^{F46}$) in vitro (*27*). During the course of establishing the expression system, we found clones for two MIIB cDNAs having slightly different sequences. In this paper, we describe a new isoform of nonmuscle myosin MIIB, the assembly properties of both MIIB isoforms as well as a chimera containing elements from both MIIBs, and the effects of phosphorylation by PK C and CK II on assembly of $MIIA^{F46}$ and two MIIBs. To understand the basis for the isoform-specific effects of phosphorylation, we have determined the exact phosphorylation sites for these kinases in each isoform. The results presented constitute evidence that heavy chain phosphorylation provides a rational mechanism for isoform-specific control of nonmuscle myosin assembly.

MATERIALS AND METHODS

Materials. Rabbit brain poly(A)$^+$ RNA and rabbit genomic DNA were purchased from Clontech (Palo Alto, CA). Vent polymerase and restriction enzymes were purchased from New England Biolabs (Beverly, MA). T4 ligase and reverse transcriptase were purchased from Gibco BRL (Gaithersberg, MD). Agarose was obtained from IBI (New Haven, CT). [γ-^{32}P]-ATP was purchased from ICN (Costa Mesa, CA). TPCK-treated trypsin, thermolysin, L-α-phosphatidyl-L-serine (PS) (from bovine brain), and ATP were from Sigma (St. Louis, MO). Lysylendopeptidase was from Wako Chem (Tokyo, Japan). CK II was purified from bovine brains as described previously (*28*) and had a specific activity of 60 nmol mg^{-1} min^{-1} at 30 °C using casein as a substrate. PK C (containing α, β, and γ isoforms as major components) was purified from rat brains by the method in ref *29* and had a specific activity of 1.1 μmol mg^{-1} min^{-1} at 37 °C in a mixed micellar assay (*30*) using histone III-s as a substrate.

Expression of Heavy Chain Fragments in E. coli. Expression and purification of human $MIIA^{F46}$ and rabbit $MIIB^{\alpha F47}$ (previously called $MIIB^{F47}$) have been described (*26, 27*). When $MIIB^{F47}$ (both α and β; see Results) was expressed, two fragments of 47 and 34 kDa were made by the bacteria (*27*). Amino acid sequence analysis of the 34-kDa fragment revealed that it started at Leu-111 (codon ^{331}CTG^{333}) of the 47-kDa fragment. To suppress initiation at this site, silent mutation of the sequence ^{328}AAACTG^{333} to ^{328}AAGCTT^{333}, which generated a *Hin*dIII site, was carried out by PCR; a piece of DNA containing bases 1−340 was generated using vent polymerase, plasmid DNA containing $MIIB^{F47}$, a sense primer-A: 5′-CTAGGATCCAT**ATG**AAG GCCCAGTTC-GAGCG-3′ containing a *Bam*HI site (underlined), and an antisenseprimer: 5′-GGCTCTT**A**AGCTTCTTCTCACTCTC-3′ containing a *Hin*dIII site (underlined). In the sense primer, bases 12−14 represent the initiation codon (bold), while in the antisense primer, base 8 (bold) corresponds to base 333 of the MIIB expression plasmids. Similarly, a piece of DNA containing bases 316−1218 was made using a sense primer (5′-GAGAGTGAGAAGAAGCT**T**AA GAGCC-3′) containing a *Hin*dIII site (underlined) and an antisense primer (5′-CTAGTCGACATGTTGATCTTTCGTAAGGAGTC-3′) containing a *Sal*I site (underlined). In the antisense primer, bases 12−32 correspond to bases 1612−1632 of rabbit SM_{emb} (*11*). After purifying the PCR products by using Wizard PCR preps (Promega, Madison, WI), the two pieces of DNA were restricted, repurified, and ligated into the *Bam*HI−*Sal*I site of pND-R. This mutation was carried out for both $MIIB^{\alpha F47}$ and $MIIB^{\beta F47}$ and for the $MIIB^{\beta/\alpha F47}$ chimera (see below).

Confirmation of Two MIIB Isoforms. Poly(A)$^+$-RNA was prepared from a single rabbit brain, reverse transcribed, and the resultant cDNA was used as a template for PCR using the 5′-primer (5′-ATGGGATCC**G**AAGCTACACGTGC-CAAC-3′) containing a *Bam*HI site (underlined) and the 3′-primer (5′-CTAGAATTCAT**G**TTGATCTTTCGTAAGGA-GTC-3′) containing an *Eco*RI site (underlined). The **G** in the 5′-primer corresponded to base 1249 while the **G** in the

3′-primer corresponded to base 1632 of rabbit SM_{emb} (*11*). This set of primers gave a product having 404 base pairs. The PCR-generated DNA was purified, restricted with *Bam*HI and *Eco*RI, repurified, and ligated into the *Bam*HI−*Eco*RI site of pUC-18u. Twenty colonies were selected. The plasmids were purified by using Wizard Plus Miniprep (Promega, Madison, WI), subjected to *Apa*I digestion (see Results), and analyzed by agarose gel. DNAs from 10 colonies were also sequenced. For sequencing of the corresponding region of genomic DNA, PCR was carried out using the same set of primers used for PCR of cDNA (above) and 1 ng of rabbit genomic DNA as template. The PCR-generated DNAs were ligated into pUC-18u and sequenced. DNA sequencing was carried out commercially using an automated fluorescent DNA sequencer (BioServe Biotechnologies, Laurel, MD).

Construction of a Chimera. A chimera comprising the nonhelical domain of $MIIB^{\alpha F47}$ and the helical domain of $MIIB^{\beta F47}$ was made as follows. First, a 1092 base pair piece of cDNA encoding amino acid residues 1−357 of $MIIB^{\beta}$ was generated by PCR using the expression plasmid for $MIIB^{\beta F47}$ as the template, a sense primer-A (see above), and an antisense primer (5′-CACGCCTC A**A**CCGGTTCT-TCAGGGTGC-3′). The latter corresponds to bases 1340−1366 of the SM_{emb} sequence (*11*), except that base 1357 was changed from G to A. This change introduced an *Age*I restriction site (underlined) without changing the amino acid of the affected codon (Leu). The cDNA coding for the nonhelical domain of $MIIB^{\alpha}$ was made by PCR using the expression plasmid for $MIIB^{\alpha F47}$ as the template. The sense primer was 5′-ATGAGAC<u>ACCGGT</u>TGAGGCGTGGGGGC-3′ whose bases 8−27 correspond to bases 1352−1371 of the SM_{emb} (*11*), except that base 13 was changed from C to **T** creating an *Age*I restriction site (underlined). The antisense primer was 5′-ATG<u>AAGCTT</u>GACT**TCA**TTCGGACTGG-3′. The underlined segment is a *Hin*dIII restriction site, and the bold letters denote the termination codon. Bases 10−26 in the 3′ primer correspond to bases 1494−1510 of the SM_{emb} (*11*). The two DNAs were ligated into pNDR between the *Bam*HI and *Hin*dIII sites, and positive clones were selected. The modified plasmid (pNDR-$MIIB^{\beta/\alpha F47}$) was expressed in *E. coli* (BL21[DE3]pLysS) as described previously (*26, 27*). The purified protein was dissolved in 6 M urea and kept at −70 °C until use. Protein concentrations were determined by the method of Lowry et al. (*31*) using BSA as a standard, unless otherwise indicated.

Phosphorylation Assay. Phosphorylations by CK II were carried out in the presence of [γ-^{32}P]ATP at 30 °C essentially as described previously (*23, 26*), while the reaction by PK C was performed in the presence of 0.2 mM PS liposomes as described previously (*27*). For assembly studies, phosphorylation of the fragments (1.0 mg) was performed in a final volume of 2.5 mL in the presence of 0.5 mM cold ATP. Aliquots from each mixture were incubated with 0.5 mM [γ-^{32}P]ATP instead of cold ATP for measurement of the phosphorylation levels. Phosphorylation levels of each sample were determined by taking aliquots (10 μg of protein) from the reaction mixtures and measuring the radioactivities associated with the acid-insoluble fractions collected on glass fiber filters as described previously (*23, 28*). When the phosphorylation reaction reached a plateau (CK II incorporated 0.8−1.1, 2.8−3.6, and 1.8−2.0 mol of phosphate/mol of $MIIA^{F46}$, $MIIB^{\alpha F47}$, and $MIIB^{\beta F47}$, respectively, while PK C incorporated 0.8−1.3 and 1.6−2.0 mol of phosphate/mol of $MIIB^{\alpha F47}$ and $MIIB^{\beta F47}$, respectively), the mixtures were brought up to 20 mM EDTA to stop the reactions. The heavy chain fragments were precipitated, washed with 66% EtOH, solubilized with a small volume of 6 M guanidine hydrochloride, and renatured by dialysis against buffer A (0.6 M NaCl, 10 mM imidazole hydrochloride at pH 7.5, 1 mM EDTA, 0.1 mM EGTA, and 0.1 mM DTT) containing 25 mM NaF as a phosphatase inhibitor as described previously (27). Nonphosphorylated controls were treated similarly, except that no kinase was added.

Isolation of Phosphopeptides. Substrate protein (1 mg) was incubated with either CK II or PK C in the presence of [γ-^{32}P]ATP in a final volume of 2.5 mL as described above. After reaching plateau levels of ^{32}P incorporation, proteins were precipitated by the addition of 10% TCA. The acid-insoluble fractions were washed extensively by 5% TCA followed by two ether washes to remove TCA. The pellets were solubilized in 2 mL of either 0.2 M NH_4HCO_3 or 10 mM Tris-HCl (pH 8.0) and were subjected to proteolysis by trypsin, thermolysin, or lysylendopeptidase. The digests were lyophilized, and the phosphopeptides were dissolved in 10 mL of 0.1 M acetic acid. The acid-soluble fractions were subjected to an iron affinity column followed by stepwise elution with buffers at various pH values as described previously (*32, 23*). A majority of the radioactivity was eluted from the columns at pH 8.3. These fractions were dried by speed vac, dissolved in 10% acetic acid (unless otherwise indicated), and applied to HPLC using a reverse-phase C-18 column (4.6 mm × 25 cm) with an acetonitrile gradient from 7.5 to 30% in 0.1% TFA over 40 min.

Localization of the Phosphorylation Sites. Aliquots of the isolated phosphopeptides were dissolved in 1 or 10% trifluoroacetic acid (TFA) and cross-linked to Sequelon AA membranes (Perceptive Biosystems, Framingham, MA) as instructed by the manufacturer. Manual Edman degradation of the cross-linked phosphopeptides was carried out on the membranes by the method of Sullivan and Wong (*33*). In our studies, all reactions were carried out in 2-mL microcentrifuge tubes instead of 1.5-mL tubes as originally described. Two-milliliter tubes allowed the Sequelon membrane disks to be positioned close to the tube bottoms, permitting the volumes of all solutions to be decreased to 125−150 μL. After each cycle of degradation, the TFA extracts were spotted directly on 3 MM filter paper (Whatman) and dried over a block heater, covered by aluminum foil, at 70 °C. The radioactivities on the filter papers were measured by a liquid scintillation counter in 10 mL of toluene−0.1% DPO. Separate aliquots of the isolated phosphopeptides were applied to an amino acid sequencer (ABS Model 470A) as well as to an amino acid analyzer. The phosphoamino acid analyses were performed by high-voltage electrophoresis at pH 1.9 at 1000 V for 90 min by the method in ref *34* using silica gel 60 plates (Alltech, Deerfield, IL) followed by autoradiography.

RESULTS

Nonmuscle Myosin II Isoforms. cDNA sequencing confirmed that the deduced amino acid sequence of $MIIA^{F46}$

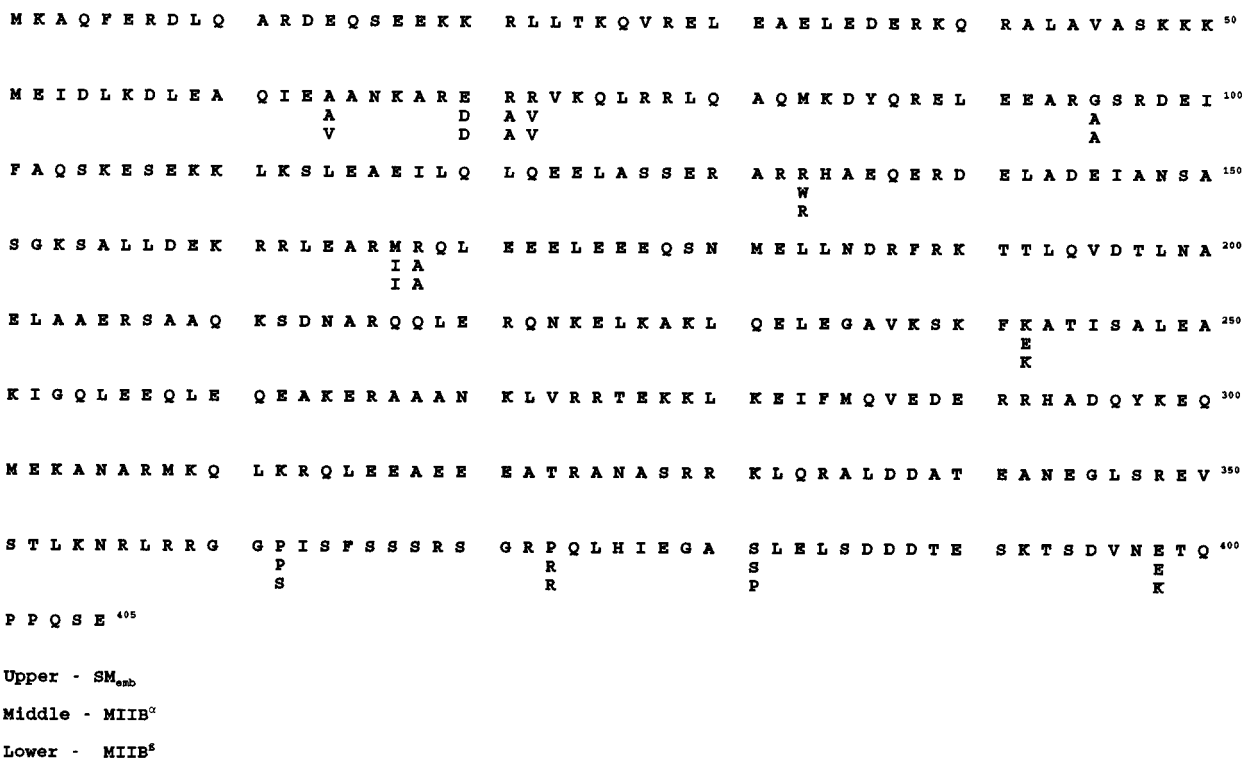

FIGURE 2: Comparison of the amino acid sequences of MIIB$^{\alpha F47}$ and MIIB$^{\beta F47}$ with SM_{emb}. The amino acid sequences of rabbit SM_{emb} reported in ref *11* is compared with the myosins studied here, which are identical with SM_{emb} except where letters are shown. First line, SM_{emb}; second line, MIIB$^{\alpha F47}$; third line, MIIB$^{\beta F47}$. The sequences correspond to residues 97−501 of SM_{emb} and residues 1572−1976 of human nonmuscle myosin B (*12*).

(generated from a human thymus cDNA preparation) was identical with that of the corresponding region of human macrophage myosin (*2*). However, we found two different MIIB clones containing closely related, but distinct, cDNA sequences. These two species of MIIB were designated MIIB$^{\alpha}$ and MIIB$^{\beta}$, for the sequence most closely related to SM_{emb} (*11*) and the new form, respectively. cDNAs coding for both forms were sequenced, and the deduced amino acid sequences are summarized in Figure 2. To confirm the existence of both MIIB sequences and to measure their relative abundance in rabbit brains, we obtained another cDNA preparation by reverse transcribing a new batch of poly(A)$^+$ RNA prepared from a single rabbit brain (whole) and carried out PCR with two primers designed to give a 404 base pair DNA that included the coding region for the entire nonhelical tailpiece. Inspection of the cDNA sequences of MIIB$^{\alpha}$ and MIIB$^{\beta}$ revealed that MIIB$^{\alpha}$ contains an *Apa*I site (GGGCCC) at the position 1368−1373 of SM_{emb} (*11*) and that MIIB$^{\beta}$ has a C → T change within this site, resulting in a Pro^{362} → Ser^{362} substitution (Figure 2) and abolishing the *Apa*I restriction site. Plasmid DNAs were isolated from 20 clones and digested by *Apa*I. Eighteen samples were cut and two were not. Eight of the clones cut by *Apa*I as well as the two that were not were sequenced. All of the clones that were cut had identical MIIB$^{\alpha}$ DNA sequences, while the two clones that were not cut by *Apa*I had the same DNA sequences as that of MIIB$^{\beta}$. These results show that both variants are indeed present in rabbit brain and that MIIB$^{\alpha}$ is the predominant form while MIIB$^{\beta}$ is a minor component representing about 10% of the MIIB expressed in rabbit brain (whole). This result suggested that rabbits possess two closely related MIIB genes. To test this, we performed PCR using rabbit genomic DNA as the template and the same primer set used above for PCR to generate a 404 base pair fragment from cDNA. The PCR product, which was the same size as that obtained using cDNA, was ligated into pUC-18u to sequence their DNA. Four clones contained the sequence seen in MIIB$^{\beta}$ while three had the DNA sequence of MIIB$^{\alpha}$. The combined results indicate that rabbits have two MIIB genes and that the predominant form expressed in rabbit brains is B$^{\alpha}$.

Assembly Properties of MIIB$^{\alpha F47}$ and MIIB$^{\beta F47}$. The three substitutions within the nonhelical domain (Ser^{362} ↔ Pro^{362}; Pro^{381} ↔ Ser^{381}; Lys^{398} ↔ Glu^{398}) between MIIB$^{\alpha}$ and MIIB$^{\beta}$ (Figure 2) seemed to have the potential to affect the structure of this region and thus to alter the assembly properties of the two MIIB isoforms. Therefore, assembly of MIIA^{F46}, MIIB$^{\alpha F47}$, and MIIB$^{\beta F47}$ was measured at various NaCl concentrations (Figure 3). In the absence of Mg^{2+}, after microcentrifugation for 30 min, 50% of the MIIB$^{\beta F47}$ was recovered in the supernatant at about 145 mM NaCl while 50% of the MIIB$^{\alpha F47}$ and MIIA^{F46} was recovered in the supernatant at about 190 and 180 mM NaCl, respectively. $MgCl_2$ at 5 mM augmented assembly of MIIB$^{\alpha F47}$ and MIIB$^{\beta F47}$; the NaCl concentrations required for 50% recovery of protein in the supernatants increased to about 165 and 205 mM for MIIB$^{\beta F47}$ and MIIB$^{\alpha F47}$, respectively. In the case of MIIA^{F46}, $MgCl_2$ at 5 mM caused a slight inhibition of assembly; the NaCl concentration required for 50% recovery in the supernatant decreased from about 180 to 165 mM. Thus, each heavy chain fragment gave a different pattern for salt dependence of filament formation, and it was particularly noteworthy that MIIB$^{\alpha F47}$ and MIIB$^{\beta F47}$ were distinctly different, with and without $MgCl_2$. Ultracentrifugation of aliquots of the samples at 90000*g* for 20 min did not significantly alter the recovery patterns indicating that

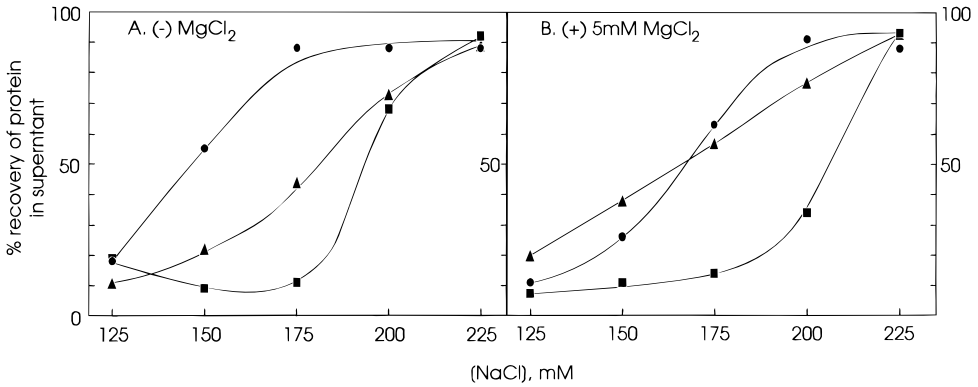

FIGURE 3: Assembly of MIIA^{F46}, MIIB$^{\alpha F47}$, and MIIB$^{\beta F47}$. Heavy chain preparations stored in 6 M urea were first dialyzed against 10 mM imidazole hydrochloride (pH 7.5), 0.6 M NaCl, 1 mM EDTA, 0.1 mM EGTA, and 5 mM 2-mercaptoethanol (buffer A) and then against 50 mM NaCl, 10 mM imidazole hydrochloride (pH 7.0), 10 mM $MgCl_2$, and 0.1 mM EGTA to induce the fragment assembly. The assembled protein was precipitated by centrifugation at 24000*g* for 10 min, dissolved in Buffer A, and centrifuged again at 24000*g* for 30 min. The protein concentration of the resultant supernatant was adjusted to 0.5 mg/mL heavy chain. Forty micrograms of the protein (about 0.85 μM heavy chain dimer) was incubated in 10 mM imidazole hydrochloride (pH 7.5), 0.1 mM EGTA, with either 1 mM EDTA or 5 mM $MgCl_2$, and various concentrations of NaCl, in a final volume of 0.5 mL in microcentrifuge tubes. The reaction mixtures were incubated on ice for 4 h and then centrifuged at 13600*g* for 30 min. The 200 μL of the supernatant was removed for measurement of the protein remaining in the supernatant. Percent recovery of the protein in the supernatants is shown. (A) without $MgCl_2$, (B) with 5 mM $MgCl_2$, (▲) MIIA^{F47}, (■) MIIB$^{\alpha F47}$, (●) = MIIB$^{\beta F47}$. Note that addition of Mg^{2+} moves the curves for MIIB$^{\alpha}$ and MIIB$^{\beta}$ to the right and that for MIIA to the left.

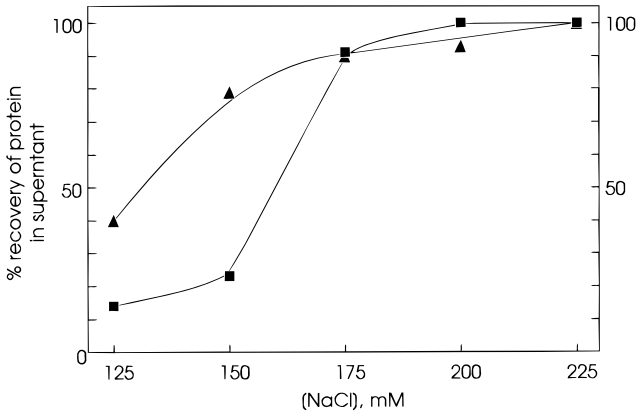

FIGURE 4: Assembly of the chimera MIIB$^{\beta/\alpha F47}$. Assembly studies were performed as described in Figure 3. (▲) without $MgCl_2$, (■) with 5 mM $MgCl_2$.

the fragments recovered in the supernatants after microcentrifugation were mostly monomers and/or small oligomers (data not shown).

To examine the factors responsible for the differences in the assembly properties between two MIIB isoforms, a MIIB$^{\beta/\alpha}$ chimera having a helical domain (amino acid residues 1−357) derived from MIIB$^{\beta F47}$ and a nonhelical domain (residues 358−405) from MIIB$^{\alpha F47}$ was constructed. Differences between MIIB$^{\alpha F47}$ and MIIB$^{\beta F47}$ include Trp^{133} ↔ Arg^{133} and Glu^{242} ↔ Lys^{242} within the α-helical coiled-coil domain and the three replacements at positions 362, 381, and 398 within the nonhelical tail end domain (see above, Figure 2). The assembly properties of the chimera were studied with and without Mg^{2+} at various salt concentrations (Figure 4). Fifty percent recovery of the chimera was seen in the supernatant at about 135 and 160 mM without $MgCl_2$ and with 5 mM $MgCl_2$, respectively. Thus, the assembly profile of the MIIB$^{\beta/\alpha F47}$ chimera was very much like that of MIIB$^{\beta F47}$ rather than that of MIIB$^{\alpha F47}$.

Phosphorylation of MIIA^{F46}, MIIB$^{\alpha F47}$, and MIIB$^{\beta F47}$. The extents of phosphorylation of MIIA^{F46}, MIIB$^{\alpha F47}$, and MIIB$^{\beta F47}$ were determined after incubation for various periods with CK II and PK C (Figure 5). CK II incorporated almost 4 mol of phosphate/mol of MIIB$^{\alpha F47}$ peptide after 90 min (thus 8 mol of phosphate/mol of two-chain coiled-coil). Under the same conditions, 1.5 and 2.0 mol of phosphate were incorporated per mole of MIIA^{F46} and MIIB$^{\beta F47}$, respectively (Figure 5A). In the case of PK C, the phosphorylation level of MIIB$^{\alpha F47}$ reached a plateau after 30−60 min of incubation, at about 1 mol of phosphate/mol of heavy chain peptide. In contrast, under the same conditions, PK C incorporated slightly over 2 mol of phosphate/mol of MIIB$^{\beta F47}$ (Figure 5B). Consistent with our previous studies (*26*, *27*), the extent of phosphorylation of MIIA^{F46} by PK C was significantly lower (less than 0.5 mol/mol MIIA) than of the MIIB isoforms.

Effects of Phosphorylation on Assembly of the Heavy Chain Fragments. Our previous studies showed that assembly of MIIB$^{\alpha F47}$ was completely inhibited after phosphorylation by PK C up to 1 mol/mol heavy chain (*27*). Consistent with this, phosphorylation by PK C completely inhibited assembly of MIIB$^{\alpha F47}$ (Figure 6B) while phosphorylation of MIIA^{F46} up to 0.5 mol/mol heavy chain did not affect its assembly over the entire range of NaCl concentrations (Figure 6A). PK C-mediated incorporation of 2 mol of phosphate/mol of MIIB$^{\beta F47}$ peptide completely inhibited its assembly (Figure 5C). The pattern was indistinguishable from that of MIIB$^{\alpha F47}$ (Figure 6B,C), despite the differences in the extent of phosphate incorporation between these two MIIB isoforms.

The effect of phosphorylation by CK II was also studied under similar conditions. Again, incorporation of 1 mol phosphate/mol of MIIA^{F46} peptide did not affect its assembly (Figure 6A). In the case of MIIB$^{\alpha F47}$, CK II phosphorylation (4 mol/mol peptide) strongly inhibited assembly; the level of the inhibition was very similar to that caused by PK C phosphorylation (Figure 6B). In contrast, CK II phosphorylation of MIIB$^{\beta F47}$ (2 mol/mol peptide) had only a minor effect on its assembly (Figure 6C).

Localization of the PK C and CK II Phosphorylation Sites. The results in Figure 6 demonstrate the isoform-specific effects of phosphorylation on assembly of the fragments of

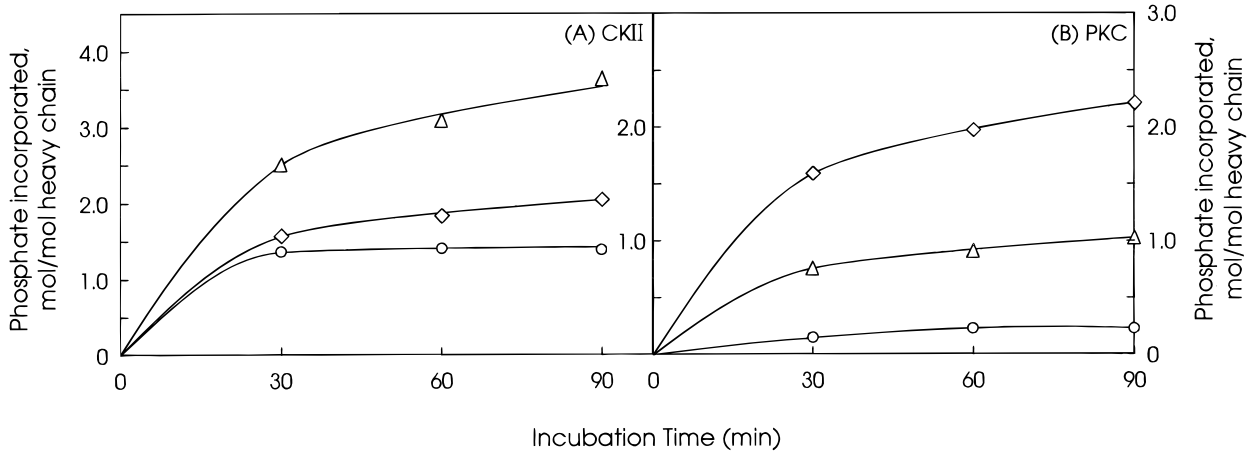

FIGURE 5: Time course of phosphorylation of MIIA^{F46}, MIIB$^{\alpha F47}$, and MIIB$^{\beta F47}$ by CK II (A) and PK C (B). Phosphorylation of heavy chain fragments (10 μg) by CK II (0.5 μg) was carried out in the presence of 40 mM imidazole hydrochloride (pH 7.5), 0.2 mM EGTA, 5 mM $MgCl_2$, 0.1 mM DTT, and 0.15 M NaCl in a final volume of 0.1 mL. Phosphorylation of the protein by PK C (0.3 μg) was carried out in the presence of 40 mM Tris-HCl (pH 7.5), 0.15 M NaCl, 0.1 mM DTT, 5% glycerol, 2 mM phosphatidylserine as liposomes, 5 μg/mL leupeptin, and 0.1 mM [γ-^{32}P]-ATP. The latter reaction was initiated, after 20 min of preincubation (see ref *27*), by addition of $CaCl_2$ and $MgCl_2$ to 0.2 and 5 mM, respectively. At each point, the reactions were terminated by the addition of 3 N H_2SO_4−4% silicotungstate. The protein-bound radioactivity was collected on glass fiber filters and counted as in ref *23*. The specific phosphate incorporation into the peptide was calculated by subtracting the radioactivity incorporated into the kinase fraction from the total amount of ^{32}P phosphate incorporated into proteins incubated with the kinase. (○) MIIA^{F46}, (△) MIIB$^{\alpha F47}$, (◇) MIIB$^{\beta F47}$.

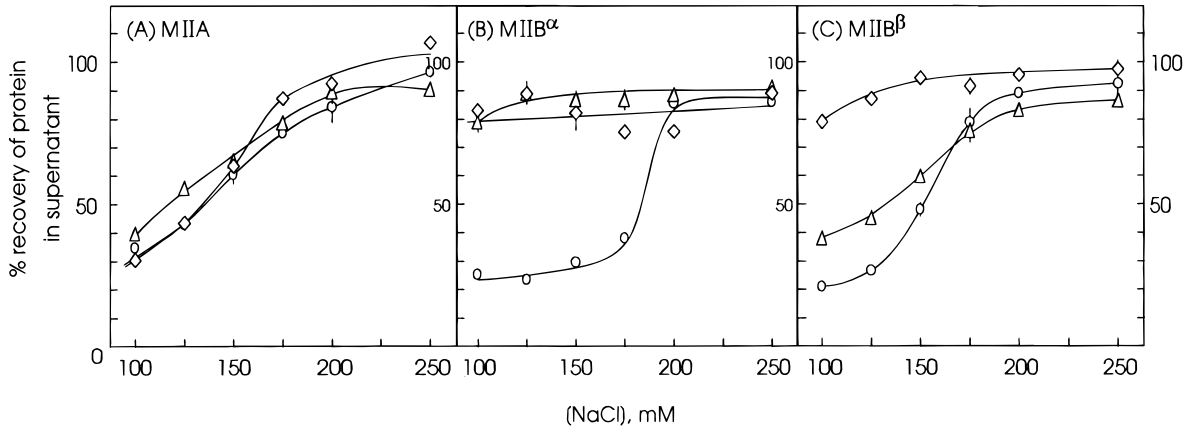

FIGURE 6: Effects of phosphorylation on assembly of MIIA^{F46} (A), MIIB$^{\alpha F47}$ (B), and MIIB$^{\beta F47}$ (C). The heavy chain fragments (70 μg/mL) were incubated at 4 °C overnight in a buffer containing 10 mM imidazole hydrochloride (pH 7.5), 1 mM EDTA, 0.1 mM EGTA, 25 mM NaF, and various concentrations of NaCl in a final volume of 0.3 mL. Aliquots of the incubation mixtures were centrifuged as in Figure 3. Protein contents in the solutions were measured before and after centrifugation using Coomassie Blue dye as described previously (*27*) and MIIA^{F46} or MIIB$^{\alpha F47}$ as a standard. It should be noted that the incubation conditions used in Figure 3 and in this figure were not the same; here, 25 mM NaF was included to inhibit phosphatases to avoid dephosphorylation during the assembly test. (○) unphosphorylated control; (△) phosphorylated by CK II; (◇) phosphorylated by PK C.

the nonmuscle myosin heavy chains. To understand the basis for these isoform specific effects, we attempted to identify all phosphorylation sites in each heavy chain fragment. Phosphoamino acid analysis revealed that CK II phosphorylated both Ser and Thr residues in all three heavy chain isoforms with serine being the major amino acid phosphorylated and that PK C phosphorylated only serine(s) (Figure 7). Addition of heparin, a specific inhibitor of CK II, at 0.2 mg/mL significantly reduced the incorporation of ^{32}P phosphate into both Ser and Thr. Also, substitution of [γ-^{32}P]-ATP with [γ-^{32}P]GTP (*35*) did not affect the incorporation rates of ^{32}P phosphate, nor did it alter the ratio of Ser to Thr phosphorylation (data not shown). Therefore, the above phosphorylation reactions seemed indeed to be mediated by CK II, not by another kinase(s) contaminating the kinase preparation. Since PK C and CK II affected the assembly of the MIIB, but not MIIA (Figure 6), in the following sections we describe the phosphorylation sites in the MIIB isoforms.

The CK II Sites in MIIB$^{\alpha F47}$. To isolate peptides containing the CK II sites, we first digested the ^{32}P-labeled MIIB$^{\alpha F47}$ with trypsin. A representative HPLC pattern of the tryptic peptides retained by an iron affinity column is shown in Figure 8A. The peptide peaks were collected, and the amounts of radioactivity were measured. Most of the radioactivity was eluted (1) between 19 and 23 min and (2) between 30 and 36 min as seen in the figure. Aliquots of each radioactive fraction were subjected to phosphoamino acid analysis. Most fractions contained both phosphoserine and phosphothreonine; ^{32}P-Ser was the major and ^{32}P-Thr was the minor phosphoamino acid. The overall recoveries of ^{32}P phosphate are summarized in Table 1.

Based upon the amounts and types of PTH-amino acids recovered after each cycle of Edman degradation and the

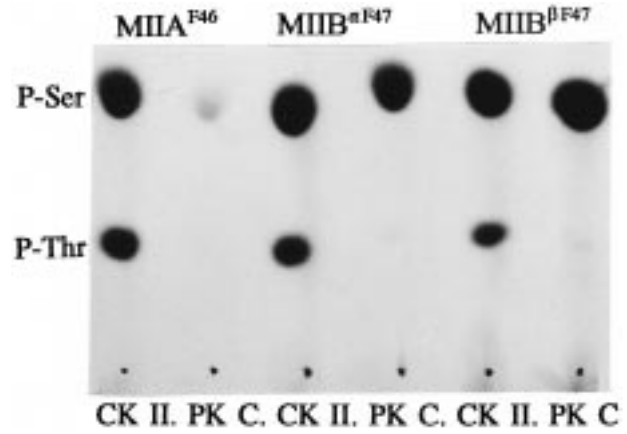

FIGURE 7: Phosphoamino acid analysis of MIIA^{F46}, MIIB$^{\alpha F47}$, and MIIB$^{\beta F47}$ phosphorylated by CK II and PK C. Phosphoamino acid analyses were performed as described in Materials and Methods. P-Ser, phosphoserine; P-Thr, phosphothreonine.

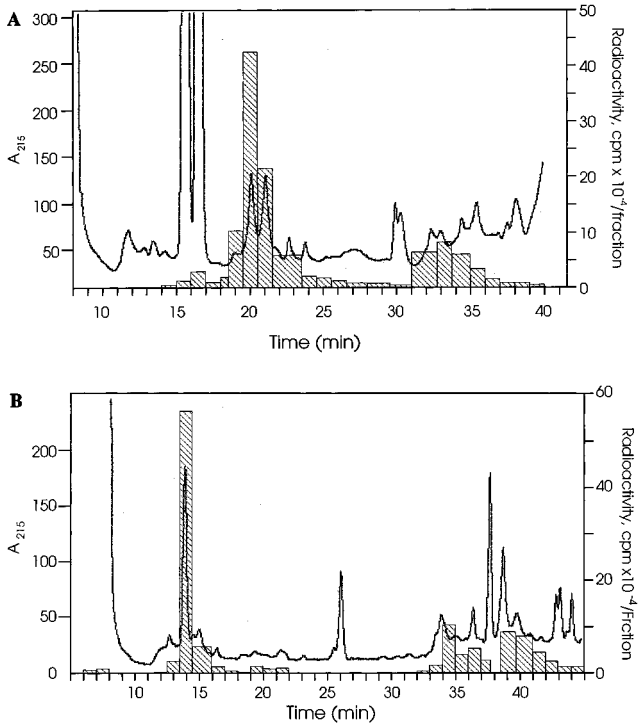

FIGURE 8: Isolation of phosphopeptides by HPLC after digestion by trypsin (A) and lysylendopeptidase (B) of MIIB$^{\alpha F47}$ phosphorylated by CK II. The CK II-phosphorylated protein (1 mg), dissolved in 3 mL of 0.2 M sodium bicarbonate, was digested by TPCK-treated trypsin by adding 0.5 mg of the enzyme three times over a 36-h incubation period. Excess trypsin was added to drive the digestion to completion. For lysylendopeptidase digestion, the phosphorylated MIIB$^{\alpha F47}$ was dissolved in 10 mM Tris-HCl (pH. 7.5) and incubated with the enzyme (10 μg) at 37 °C for 16 h. The digests were lyophilized and applied to an iron affinity column; the radioactive fractions were eluted by ammonium acetate at pH 8.3. These fractions were dried, redissolved in a small volume of 10% acetic acid, and subjected to HPLC using an acetonitrile gradient from 7.5 to 30% in 0.1% TFA between 5 and 40 min. Fractions corresponding to peaks were collected. The two A_{215} peaks seen between 15 and 17 min are derived from solvent artifacts. Aliquots were taken for measurement of radioactivity.

known sequence of MIIB$^{\alpha F47}$, the amino acid sequence of each peptide isolated by HPLC was determined. The same sequence, X(Ser)-L-E-L-X-, was identified at the beginning of all tryptic peptides from MIIB$^{\alpha F47}$. They were clearly derived from the nonhelical domain, as expected from our previous study of bovine brain myosin (*23*). The tryptic peptides recovered from Frac-19−23 were subjected to manual Edman degradation (*33*) to identify the exact phosphorylation site(s). Peptides eluted as Frac-19$_{Tryp}$ (tryptic fragments eluted between 18 and 18.30 min) and Frac-20$_{Tryp}$ (18.30−19.30 min) released free ^{32}P phosphate at three positions, the first, fifth, and ninth cycles, while the peptides recovered in Frac-21$_{Tryp}$ (19.30−20.30 min) and Frac-22$_{Tryp}$ (20.30−21.30 min) released ^{32}P phosphate at the 5th, 9th, and 14th cycles (Figure 9A−D). The amounts of phosphate released after the first cycle were much smaller with these fractions than with Frac-19$_{Tryp}$ and Frac-20$_{Tryp}$. Since yields decrease in proportion to the number of cycles, the radioactivity released at cycles 9 and 14 are high enough to identify them as the phosphorylation sites. The peptide(s) recovered in Frac-23/24$_{Tryp}$ (21.30−23.30 min) released radioactivity mainly at cycle 5, and minor amounts were released at cycles 9 and 14 (Figure 9E). To confirm the release of free phosphate (and not phosphopeptide) after the first cycle, in a separate set of experiments, aliquots of the TFA extracts from the first and fifth cycles were subjected to high-voltage electrophoresis using a silica gel plate to measure the free and peptide-bound forms of ^{32}P phosphate. Most of the radioactivity recovered in both cycles was indeed in the form of free phosphate, confirming the first Ser as a CK II site. Thus, we concluded that the CK II phosphorylation sites are S(PO$_4$)-L-D-L-S(PO$_4$)-D-D-D-T(PO$_4$)-E-S-K-T-S(PO$_4$)-D- for peptides in Frac-19−23. Amino acid analysis showed that the peptides in Frac-19$_{Tryp}$−23$_{Tryp}$ were longer than 15-mers. However, it was difficult to identify any sites beyond the 15 cycles. Trypsin did not efficiently cleave the peptide bond between Lys and Thr in the CK II-phosphorylated MIIB$^{\alpha F47}$. We therefore subjected a new preparation of MIIB$^{\alpha F47}$ ^{32}P-labeled by CK II to lysylendopeptidase digestion. Approximately 25% of the radioactivity applied to the HPLC was recovered in a single peptide peak that eluted between 13.5 and 14.5 min (Frac-14$_{LysEndo}$) (Figure 8B) (Table 1). Phosphoamino acid analysis revealed that the peptide(s) in this fraction was phosphorylated at only Ser residue(s). Amino acid sequencing and amino acid analysis indicated that this fraction contained a single peptide, T-S-D-V-N-E-T-Q-P-P-Q-S-E, while manual Edman degradation showed that this peptide was phosphorylated by CK II at two sites, the second and 12th positions (see Supporting Information). Thus we concluded that the phosphorylation sites in this peptide are T-S(PO$_4$)-D-V-N-E-T-Q-P-P-Q-S(PO$_4$)-E. Combining the foregoing results, CK II phosphorylates five sites in the nonhelical domain of MIIB$^{\alpha F47}$ (see Figure 13 for a summary).

The CK II Sites in MIIB$^{\beta F47}$. MIIB$^{\beta F47}$ was expected to be phosphorylated at the same or similar sites as MIIB$^{\alpha F47}$ because its amino acid sequence is closely related to that of MIIB$^{\alpha F47}$, and proteolytic digestions were performed with lysylendopeptidase and thermolysin. Thermolysin was chosen because (1) trypsin would be unable to cleave between Ala and Pro at the bond corresponding to the Ala-Ser that was cleaved in MIIB$^{\alpha F47}$, and (2) we did not want to generate any peptides beginning with Gln, because cyclization would block Edman degradation, and tryptic digestion would have generated a phosphopeptide starting with Gln. Thermolysin digestion of the MIIB$^{\beta F47}$ ^{32}P-labeled by CK II generated

Table 1. Summary of ^{32}P Phosphate Recoveries from the Heavy Chain Digests after Phosphorylation by CK II

	MIIB$^{\alpha F47}$		MIIB$^{\beta F47}$	
	trypsin (nmol)	lysylendopeptidase (nmol)	lysylendopeptidase (nmol)	thermolysin (nmol)
^{32}P incorporated by CK II, total	81.5	90.6	48	86
^{32}P applied to the iron affinity column[a]	82.0	88.5	55.5	50.9
^{32}P applied to HPLC	58.2	63.1	31.8	41.7
^{32}P recovered from HPLC	Frac-16 (0.5)[b]	Frac-13 (0.7)[b]	Frac-7/8 (0.6)[b]	Frac-14 (0.3)[b]
	-17 (1.0)	-14 (15.8)	-14 (6.9)	-15 (5.4)
	-19 (0.7)	-15 (1.3)	-15 (0.3)	-16 (0.7)
	-20 (3.8)	-35 (2.7)	-26 (0.2)	-22 (1.1)
	-21 (15.7)	-36 (1.3)	-34/35 (3.6)	-25 (0.6)
	-22 (7.9)	-37 (1.7)	-36 (0.8)	-26 (0.4)
	-23/24 (4.4)	-38 (1.0)	-37 (0.7)	-29 (1.4)
	-25 (0.8)	-39 (1.1)	-38 (1.1)	-30 (7.2)
	-26 (0.7)	-40 (2.8)	-39 (3.5)	-31 (4.7)
	-32/33 (4.8)	-41 (2.8)	-40 (0.4)	-32 (2.5)
	-34 (3.1)	-42 (1.3)		-36 (0.6)
	-35 (2.2)			
	-36 (1.2)			

[a] These fractions contained some residual free [^{32}P]ATP. [b]Nanomole of ^{32}P phosphate recovered in each fraction is shown within parentheses.

several major phosphopeptides that eluted from HPLC around 14−15 min (Frac-15$_{Therm}$) and between 29 and 32 min (Frac-29$_{Therm}$, -30$_{Therm}$, -31$_{Therm}$, and -32$_{Therm}$) as well as several minor peptides (Figure 10A). The peptides eluting at Frac-15$_{Therm}$, -16$_{Therm}$ (15−16 min), and -Frac-22$_{Therm}$ (21−22 min) contained only phosphoserine while those eluted in Frac-29$_{Therm}$ (28.75−29.25 min) had both phosphoserine and phosphothreonine in equal amounts. The peptides recovered in Frac-30$_{Therm}$ (29.25−30 min), -31$_{Therm}$ (30−30.7 min), and -32$_{Therm}$ (30.7−32 min) contained phosphoserine as a major and phosphothreonine as a minor phosphoamino acid. The peptide in Frac-15$_{Therm}$ was identified as V-N-K-T-Q-P-P-Q-S-E, the COOH-terminal peptide. Since Ser (not Thr) was phosphorylated in this fraction, the CK II site had to be the Ser at the second position from the COOH end. Indeed, this peptide released free phosphate at the ninth cycle of Edman degradation, confirming the Ser as the CK II site. The amino acid sequences of minor peptides in fractions that eluted between 21 and 22 min (Frac-22$_{Therm}$) and 24−24.70 min (Frac-25$_{Therm}$) were identified as L-E-L-S-D-D-D-T-E-S-K-T-S-D. The sequences of the peptides in Frac-29$_{Therm}$, -30$_{Therm}$, -31$_{Therm}$, -32$_{Therm}$, and -33$_{Therm}$ all appeared to be I-E-G-A-P-L-E-L-S-D-D-D-T-E-S-K-T-S-D. The peptides in Frac-29$_{Therm}$ released free ^{32}P phosphate at the 9th and 13th cycles of manual Edman degradation; the two sites seemed to be equally phosphorylated in the peptide. The major phosphorylation site in the peptides in Frac-30$_{Therm}$−33$_{Therm}$ was at position 9. The combined results suggest that the CK II sites are I-E-G-A-P-L-E-L-**S**(^{32}P)-D-D-D-**T**(^{32}P)-E-. To identify any CK II sites within the peptide region T-S-D-V-N-K, ^{32}P-labeled MIIB$^{\beta F47}$ was digested by lysylendopeptidase. The phosphopeptide having the sequence T-S-D-V-N-K was recovered in the pass-through fraction after the first HPLC (Figure 10B). This fraction was dried, dissolved in water, and reapplied to HPLC with an acetonitrile gradient 0−5% (5−15 min) followed by 5−20% (15−40 min). Under these conditions the peptide was recovered as a single peak eluted between 13 and 15 min. The results of amino acid sequencing and manual Edman degradation showed that the CK II site in this peptide was T-**S**(PO_4)-D-V-N-K. In summary, we found four CK II sites in MIIB$^{\beta F47}$ (Figure 13).

The PK C Sites in MIIB$^{\alpha F47}$. When tryptic phosphopeptides from the PK C-labeled MIIB$^{\alpha F47}$ were applied to HPLC, most of the radioactivity was recovered in pass-through fractions (between 7 and 9 min), at 15−16 min (Frac-16), and between 27 and 31 min (Frac-27−31) (Figure 11A). The recoveries of ^{32}P phosphate in each fraction are summarized in Table 2. The peptide eluted as Frac-16 was identified as E-V-S(PO_4)-T-L-K phosphorylated at the Ser residue since PK C phosphorylated only serine in MIIB$^{\alpha F47}$ (Figure 7). It should be noted that previous studies showed that, in MIIA, PK C phosphorylated the second Ser in the equivalent peptide, E-V-S-S(PO_4)-L-K (*25*, *26*). The tryptic peptides that eluted between 27 and 31 min could be identified as two related peptides; G-G-P-I-X-F-S- and R-G-G-P-I-X-F-S-. To avoid this complexity due to incomplete digestion by trypsin, another preparation of MIIB$^{\alpha F47}$ phosphorylated by PK C was digested by thermolysin, and its radioactive peptides were isolated by HPLC. As shown in Figure 11B, thermolysin generated one major radioactive peptide peak between 14 and 14.7 min (Frac-15$_{Therm}$), which contained 44% of the radioactivity applied (Table 2) as well as several minor phosphopeptides. In contrast to the tryptic digestion, thermolysin did not generate any detectable radioactive peptides in the pass-through fractions. The amino acid sequence of the peptide in Frac-15$_{Therm}$ was F-S-S-S-R-S-G-R-R-Q while that of Frac-20$_{Therm}$ (19.25−20.25 min) was L-R-R-G-G-P-I-S, and those of Frac-29$_{Therm}$ (28−29 min) and 30$_{Therm}$ (29−30 min) were both L-R-R-G-G-P-I-S-F-S-S-S-R-S-G-R-R-Q. The peptide in Frac-15$_{Therm}$ released free ^{32}P phosphate at three cycles, three, four, and six (Figure 12A); positions 4 and 6 were the main phosphorylation sites while position 3 was a minor site. Thus, the PK C sites in the peptide were identified as F-S-S(PO_4)-S(PO_4)-R-S(PO_4)-G-R-R-Q. The peptide in Frac 20$_{Therm}$ was phosphorylated at one position (Figure 12B), L-R-R-G-G-P-I-S(PO_4). The peptides in Frac-29$_{Therm}$ and -30$_{Therm}$, in contrast, had at least three phosphorylation sites at 8, 10, and 14 (Figure 12C,D), L-R-R-G-G-P-I-S(PO_4)-F-S(PO_4)-S-S-R-S(PO_4)-G-R-R-Q. The release of radioactivity at the first and second positions of these peptides was due to the extraction of phosphopeptides loosely bound to the Sequelon AA membrane. The combined results in Figure 12 indicate that all the Ser residues

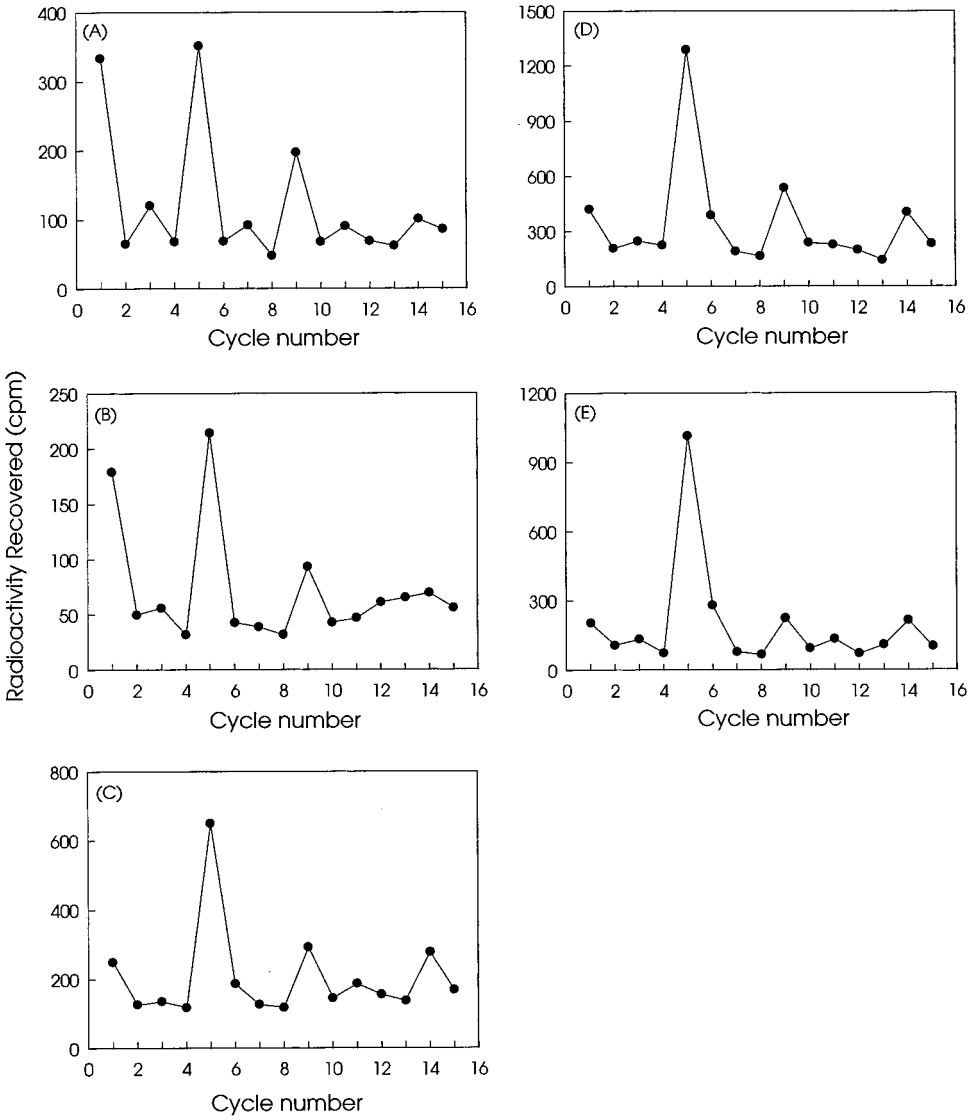

FIGURE 9: Manual Edman degradation of tryptic phosphopeptides from MIIB$^{\alpha F47}$. Aliquots of phosphopeptides isolated by HPLC (Figure 8) were used for manual Edman degradation, and the amounts of free ^{32}P phosphate extracted by TFA after each cleavage were measured. Total radioactivities originally applied to the Sequelon AA membranes were (A) Frac-19$_{Tryp}$, 20 000 cpm; (B) Frac-20$_{Tryp}$, 37 000 cpm; (C) Frac-21$_{Tryp}$, 42 000 cpm; (D) Frac-22$_{Tryp}$, 42 000 cpm; and (E) Frac-23$_{Tryp}$, 30 000 cpm.

in the cluster from residues 364−370 within the nonhelical domain of MIIB$^{\alpha F47}$ are phosphorylatable by PK C (see Figure 13 for a summary), although the extent of phosphorylation of these sites is very likely not equal.

The PK C Sites in MIIB$^{\beta F47}$. MIIB$^{\beta F47}$ ^{32}P-labeled by PK C was subjected to tryptic digestion. By HPLC, one major and two minor phosphopeptide peaks were isolated. The major peptide peak gave amino acid sequences of (±R)-G-G-S-I-S-F (see above). One of the minor peaks gave the sequence E-V-S-T-L-K while the other was (±R)-G-G-S-I-S-F-S-S-S-R. As in MIIB$^{\alpha F47}$, the PK C site in the peptide E-V-S-T-L-K was identified as the Ser residue at the third position, E-V-S(PO$_4$)-T-L-K, since only Ser was phosphorylated by PK C (Figure 7). To identify the PK C sites within the cluster of Ser residues, another preparation of the phosphorylated MIIB$^{\beta F47}$ was subjected to thermolysin digestion. As seen in Figure 11C, three major phosphopeptide peaks were isolated by HPLC, Frac-14$_{Therm}$ (12.75−13.75 min), -16$_{Therm}$ (14.30−15.30 min), and -17$_{Therm}$ (15.30−16.25 min). There was no detectable radioactivity in the pass-through fractions (up to 10 min), indicating that thermolysin did not generate small, hydrophilic phosphopeptides from the ^{32}P-labeled MIIB$^{\beta F47}$. The phosphopeptides eluted in Frac-14$_{Therm}$ and Frac-16$_{Therm}$ had the sequences L-R-R-G-G-S and F-S-S-S-R-S-G-R, respectively, while the one in Frac-17$_{Therm}$ was L-R-R-G-G-S-I-S. Since the phosphopeptide in Frac-14$_{Therm}$ contained only one serine residue, its PK C site was identified as L-R-R-G-G-S(PO$_4$). The phosphorylation sites in the peptides of Frac-16$_{Therm}$ were at two positions F-S-S-S(PO$_4$)-R-S(PO$_4$)-G-R. Position 3 of this peptide seemed to be a minor PK C site. In contrast, only one phosphorylation site was identified in the peptide in Frac-17$_{Therm}$, L-R-R-G-G-S(PO$_4$)-I-S. Thus, three major PK C sites were localized within a cluster of Ser residues in MIIB$^{\beta F47}$; L-R-R-G-G-S(PO$_4$)-I-S-F-S-S-S(PO$_4$)-R-S(PO$_4$)-G-R. In contrast to MIIB$^{\alpha F47}$, we have no evidence for phosphorylation of two of the Ser residues, those on either side of Phe.

Stoichiometry of Phosphorylation. Based upon the studies of the stoichiometry of phosphorylation (Figure 5), all five sites in MIIB$^{\alpha F47}$ could be fully phosphorylated by CK II.

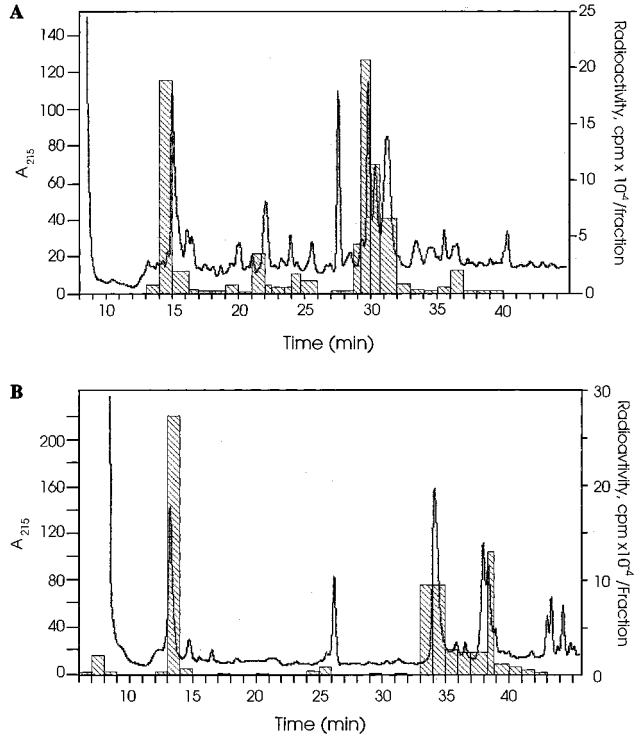

FIGURE 10: HPLC separation of the phosphopeptides from ^{32}P-labeled MIIB$^{\beta F47}$ by CK II. MIIB$^{\beta F47}$ (1 mg) was digested by thermolysin (10 μg) in the presence of 0.2 M ammonium bicarbonate (A) or lysylendopeptidase (10 μg) in 10 mM Tris-HCl (pH 7.5) (B). The phosphopeptides were recovered by HPLC as described in Figure 8.

However, the four sites in MIIB$^{\beta F47}$ do not seem to be fully phosphorylated since CK II incorporated a maximum of only 2 mol of phosphate/mol of heavy chain peptide. We therefore calculated the stoichiometries of phosphate incorporation of each peptide used above. As seen in Table 3, the tryptic peptides in Frac-19$_{Tryp}$−24$_{Tryp}$ from the CK II-labeled MIIB$^{\alpha F47}$ gave stoichiometries from 2.4 to 6, and these peptides were found to contain five CK II sites. Similarly, three phosphopeptides generated by lysylendopeptidase gave stoichiometries of 1.2−1.8 while two or three sites were phosphorylatable by CK II. For the MIIB$^{\beta F47}$ peptides, the stoichiometry of Frac-22$_{Therm}$ (three identified CK II sites) was 1.7, while those of Frac-34/35$_{LysEndo}$ and Frac-39$_{LysEndo}$ were 0.6 and 0.9, respectively (both peptides had two phosphorylatable sites). Thus, the peptides isolated from MIIB$^{\alpha F47}$ phosphorylated by CK II contained phosphate at between one and five sites, while those from MIIB$^{\beta F47}$ were indeed only partially phosphorylated at the various sites.

In contrast, PK C seemed to phosphorylate only one residue among the five potential sites in MIIB$^{\alpha F47}$, based upon the overall stoichiometry of the phosphorylation. To confirm this, we also calculated the stoichiometry of ^{32}P phosphate for each peptide containing multiple PK C sites (Table 3). For MIIB$^{\alpha F47}$, the peptides in Frac-15$_{Therm}$, -29$_{Therm}$, and -30$_{Therm}$, which had four or five identified PK C sites, gave phosphate/peptide ratios up to 1, indicating that PK C phosphorylates only one site in each chain of MIIB$^{\alpha F47}$ or two sites per molecule. In the case of MIIB$^{\beta F47}$, two thermolysin fragments (Frac-16$_{Therm}$ and -17$_{Therm}$) gave ratios of 0.6; these peptides contained three and two identified PK C sites. Although we did not obtain any phosphopeptides that contained all of the potential PK C sites within MIIB$^{\beta F47}$,

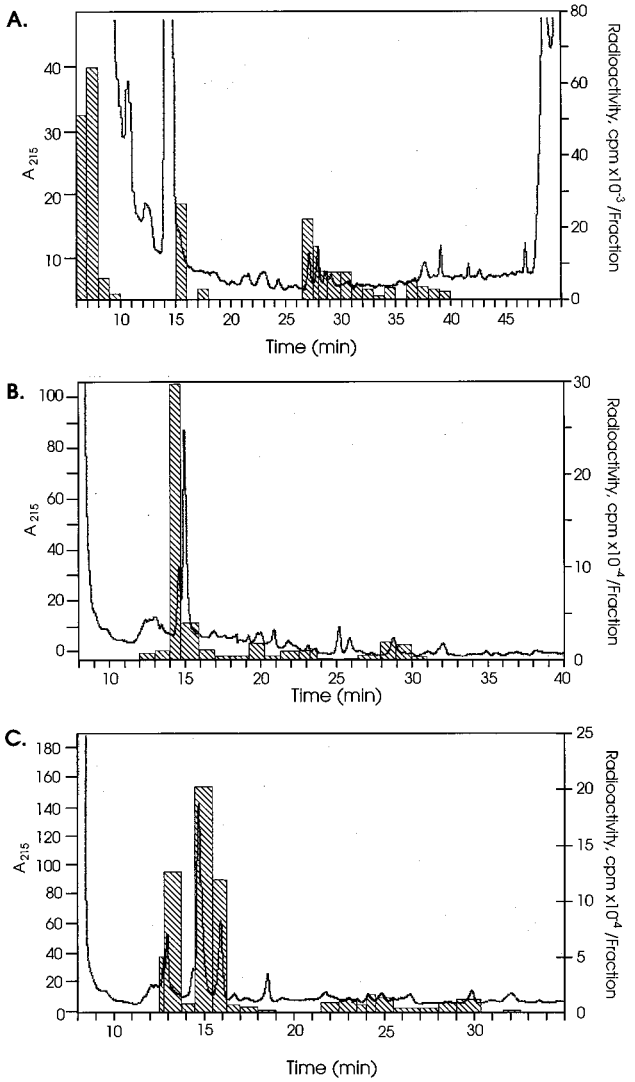

FIGURE 11: (A) and (B) HPLC separation of phosphopeptides after digestion with trypsin or thermolysin of ^{32}P-labeled MIIB$^{\alpha F47}$ by PK C. The PK C phosphorylated MIIB$^{\alpha F47}$ (1 mg) was digested by trypsin (A) or thermolysin (B) as described in Figures 8 and 10. The lyophilized samples were first dissolved in a small volume of 1.7 N acetic acid, and the extract was then diluted with H_2O to reduce the concentration to 0.1 M. To recover radioactivity efficiently from the lyophilized samples after iron affinity column chromatography, 500 μL of 50% formic acid rather than 10% acetic acid was used. In panel A, the radioactive peptide (Frac-16) was eluted at a shoulder of a large solvent peak. (C) HPLC separation of a thermolysin digest of MIIB$^{\beta F47}$ phosphorylated by PK C. The PK C-phosphorylated MIIB$^{\beta F47}$ was digested by thermolysin as in Figure 10. HPLC separation of the phosphopeptides was carried out as in Figure 8.

the extent of overall phosphorylation (2 mol/mol heavy chain) and the relative amounts of each phosphopeptide generated suggest that two out of the three potential Ser sites in each MIIB$^{\beta F47}$ heavy chain were phosphorylated by PK C (thus, at least four sites in a native MIIB$^{\beta F47}$ molecule). For both MIIB$^{\alpha F47}$ and MIIB$^{\beta F47}$, the extent of phosphorylation at E-V-S(PO_4)-T-L-K- was low relative to the overall incorporation since the recovery of this phosphopeptide was small.

PK C Site in Brain Myosin Heavy Chains. Our present study clearly identified the PK C sites at the tail end nonhelical domain of rabbit MIIB isoforms, MIIB$^{\alpha F47}$ and MIIB$^{\beta F47}$. However, studies in ref *36* showed that PK C

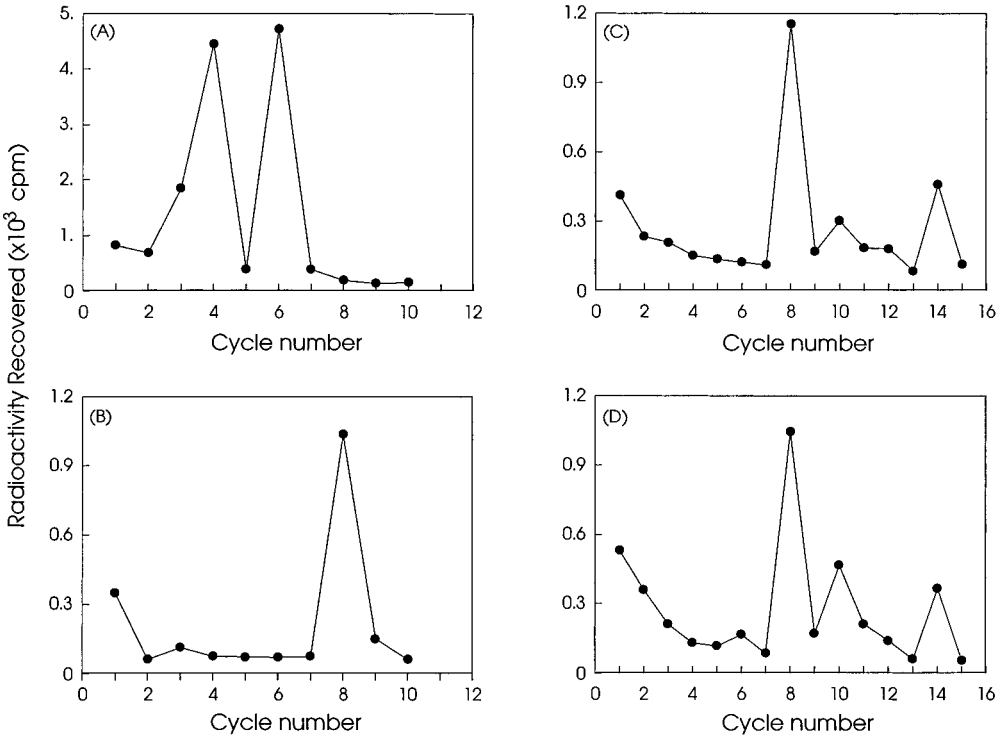

FIGURE 12: Manual Edman degradation of the phosphopeptides generated by thermolysin digestion of MIIB$^{\alpha F47}$ phosphorylated by PK C. Amounts of radioactivities applied were (A) Frac-15$_{T.M.}$, 35 000 cpm; (B) Frac-20$_{T.M.}$, 7200 cpm; (C) Frac-29$_{T.M.}$, 10 000 cpm; and (D) Frac-30$_{T.M.}$, 7200 cpm.

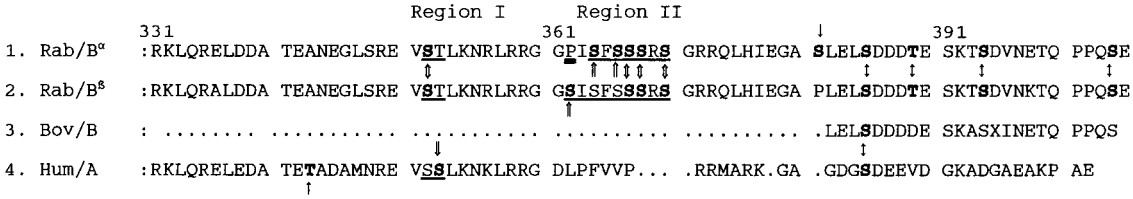

FIGURE 13: Summary of the CK II and PK C phosphorylation sites identified in MIIB$^{\alpha F47}$ and MIIB$^{\beta F47}$. Bold Ser with open arrows are the PK C sites. Bold Ser or Thr with solid arrows are the CK II sites. The Thr indicated with ↑ for human MIIA is a minor CK II site (Murakami, unpublished observation). The amino acid numbering is based upon the fragments MIIB$^{\alpha F47}$ and MIIB$^{\beta F47}$. P in MIIB$^{\alpha F47}$ is the Pro making the beginning of nonhelical tail end domain. In MIIB$^{\beta F47}$, the nonhelical domain also seems to begin in the vicinity of the residues 358−362. The X in the bovine brain sequence is probably Asp (*23*).

Table 2: Summary of ^{32}P Phosphate Recoveries from the Heavy Chain Digests after Phosphorylation by PK C

	MIIB$^{\alpha F47}$		MIIB$^{\beta F47}$
	trypsin (nmol)	thermolysin (nmol)	thermolysin (nmol)
^{32}P incorporated by PK C, total	18.7	38.5	60.1
^{32}P applied to the iron affinity column	17.8	30.0	52.0
^{32}P applied to HPLC	13.9	23.4	47.4
^{32}P recovered from HPLC	Frac -7−10 (4.4)	Frac-15 (10.3)	Frac-13 (2.4)
	-16 (1.1)	-16 (1.3)	-14 (6.0)
	-18 (0.2)	-17 (0.5)	-15 (0.8)
	-27 (0.8)	-20 (0.7)	-16 (9.5)
	-28 (0.6)	-22 (0.4)	-17 (5.6)
	-29 (0.4)	-23 (0.5)	-18 (0.5)
	-30 (0.4)	-24 (0.5)	-22 (0.6)
	-32 (0.3)	-29 (0.8)	-23 (0.7)
		-30 (0.6)	-24 (0.5)
			-25 (0.9)
			-26 (0.7)
			-30 (0.5)
			-31 (0.7)

phosphorylates bovine brain myosin within the head region, not the tail region. To confirm the major PK C site within the native MIIB myosin, we reexamined the site by using limited proteolysis of bovine brain myosin ^{32}P-labeled by PK C under our phosphorylation conditions. Because of the possibility that the proteolytic pattern of the heavy chains

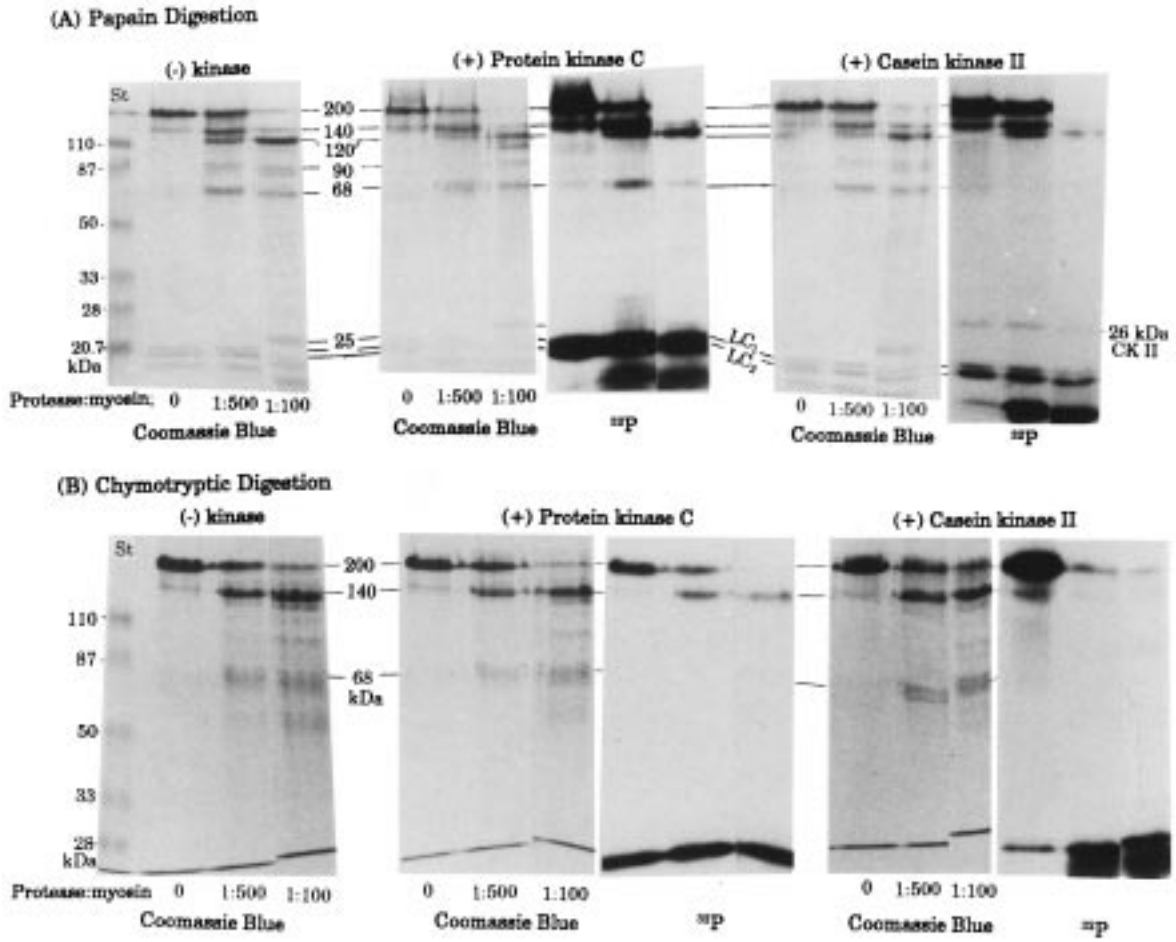

FIGURE 14: Papain (A) and chymotrypsin (B) digestion of brain myosin phosphorylated by PK C. Dephosphorylated brain myosin (25 μg) was incubated with PK C (0.9 μg) and 0.5 mM [γ-^{32}P]-ATP for 30 min at 30 °C in a final volume of 0.1 mL as described in Figure 5. The brain myosin was also incubated with CK II (1.0 μg) and 0.5 mM [γ-^{32}P]-ATP without PS liposomes as in Figure 5. After the phosphorylation reaction was terminated by the addition of 10 mM EDTA, limited proteolysis was performed by incubation with various concentrations of papain or chymotrypsin for 10 min at 30 °C. The resultant digests were subjected to SDS−12.5% PAGE followed by Coomassie Blue staining and autoradiography. PK C incorporated about 0.8 mol of phosphate/mol of heavy chain and 0.8 mol of phosphate/mol of light chains. CK II also incorporated about 0.8 mol of phosphate/mol of heavy chain.

could change after PS-liposome binding as well as phosphorylation, three sets of brain myosins were used for papain and chymotryptic digestions carried out under similar conditions used by others (*36*): (1) brain myosin incubated with neither kinase nor liposomes, (2) the myosin phosphorylated by casein kinase II, and (3) the myosin phosphorylated by PK C in the presence of PS liposomes. Phosphorylation of and PS binding to heavy chains had little effect upon the proteolytic patterns of heavy chains by these proteases (Figure 14). Papain digestion of the myosin phosphorylated by PK C generated major radioactive fragments of 140 and 120 kDa and multiple fragments smaller than 16 kDa (Figure 14A). Minor levels of radioactivity were associated with fragments of 90, 68, and 25 kDa. Papain further digested the radioactive 120-kDa fragment to a nonradioactive 110-kDa fragment. Chymotryptic digestion of the heavy chains phosphorylated by PK C produced a radioactive fragment of 140 kDa and multiple nonradioactive bands of about 68 kDa (Figure 14B). The 120-kDa fragment corresponds to the rod region, while the 90-, 68-, and 25-kDa fragments arise from the head region. The 140-kDa fragment is the 120-kDa rod fragment combined with the 25-kDa fragment at its N-terminus (*37*). Under our phosphorylation conditions, i.e., using PS liposomes and mixing myosin with PS liposomes prior to the phosphorylation reaction, the major phosphorylation site(s) by PK C in bovine brain myosin heavy chains was (were) identified to be within the rod region (120 and 140 kDa). The region containing the PK C site was eventually cleaved off by both proteases from the major rod region into fragments smaller than light chains. Meanwhile, the CK II site, localized within the nonhelical domain (*23*), was more susceptible to proteolysis than the PK C site (Figure 14A,B). Phosphoamino acid analysis revealed that PK C phosphorylated only Ser residue(s) in native brain myosin heavy chain. The results suggest that the main PK C phosphorylation site in native brain myosin heavy chains is near or within the nonhelical domain, consistent with the peptide localization described above.

DISCUSSION

We have described here two closely related isoforms of rabbit MIIB, designating the one most closely related to the previously published rabbit MIIB (SM_{emb}) as $MIIB^{\alpha}$ and the unique one as $MIIB^{\beta}$. The COOH-terminal regions of these two MIIB isoforms ($MIIB^{\alpha F47}$ and $MIIB^{\beta F47}$) as well as the corresponding region of human MIIA ($MIIA^{F46}$) differed in their assembly properties in the presence of various concentrations of NaCl and in the effect of Mg^{2+} upon assembly.

Table 3: Stoichiometries of Phosphopeptides Isolated from MIIB$^{\alpha F47}$ and MIIB^{bF47} Phosphorylated by CK II or PK C

peptide name	amount[a] (pmol)	^{32}P phosphate (pmol)	^{32}P/peptide (mol/mol)	no. of sites identified
	MIIB$^{\alpha F47}$ Phosphorylated by CK II			
Frac-19$_{Tryp}$ (X-L-E-L-X-)	98	300	3.1	5
-20$_{Tryp}$ (X-L-E-L-X-)	67	400	6.0	5
-21$_{Tryp}$ (X-L-E-L-X-)	87	450	5.2	5
-22$_{Tryp}$ (X-L-E-L-X-)	94	270	2.9	5
-23/24$_{Tryp}$ (X-L-E-L-X-)	83	200	2.4	5
Frac-14$_{LysEndo}$ (T-X-D-V-)	86	335	1.8	2
-40$_{LysEndo}$ (N-R-L-R-R-G-)	97	119	1.2	3
-41$_{LysEndo}$ (N-R-L-R-R-G-)	113	200	1.8	3
	MIIB$^{\beta F47}$ Phosphorylated by CK II			
Frac-22$_{Therm}$ (L-E-L-S-D-D-D-)	144	250	1.7	3
Frac-34/35$_{LysEndo}$ (N-R-L-R-)	636	365	0.6	2
-39$_{LysEndo}$ (N-R-L-R-R-)	410	357	0.9	2
	MIIB$^{\alpha F47}$ Phosphorylated by PK C			
Frac-15$_{Therm}$ (F-S-X-S-R-X-)	520	462	0.9	4
-19$_{Therm}$ (L-R-R-G-G-P-I-S.)	180	120	0.7	1
-29$_{Therm}$ (L-R-R-G-G-P-I-S-)	219	235	1.1	5
-30$_{Therm}$ (L-R-R-G-G-P-I-S-)	142	120	0.9	5
	MIIB$^{\beta F47}$ Phosphorylated by PK C			
Frac-16$_{Therm}$ (F-S-S-X-R-)	766	478	0.6	3
-17$_{Therm}$ (L-R-R-G-G-)	730	456	0.6	2

[a] Determined by amino acid analysis.

Using a chimera, MIIB$^{\beta/\alpha F47}$, which has the nonhelical domain of MIIB$^{\alpha F47}$ and the helical domain of MIIB$^{\beta F47}$, it was clearly shown that the intrinsic assembly properties are dictated by the helical domain. Inspection of the amino acid sequence shows that all three replacements within the helical domain of MIIB^{F47} (Ala-64 ↔ Val, Trp-133 ↔ Arg, and Glu-242 ↔ Lys) are not at the interface between the two chains of the coiled coil (a and d positions, *38*) but rather are on the surface of the coiled coil, where they can affect the intermolecular interactions that stabilize the filaments. The isoforms also differed at three positions in the nonhelical domain. Two of the changes are reciprocal Ser ↔ Pro substitutions, while the other is a Glu ↔ Lys. These substitutions lead to differences in the patterns of phosphorylation of MIIB$^{\alpha F47}$ and MIIB$^{\beta F47}$ by PK C and CK II. Ser-362, found only in rabbit MIIB$^{\beta}$, was identified as a highly phosphorylatable PK C site while Ser-381 was identified as the CK II site unique to MIIB$^{\alpha}$. These differences in phosphorylation patterns resulted in differences in their ability to assemble (Figure 6). Phosphorylation by PK C strongly inhibited the assembly of both MIIB isoforms, while CK II phosphorylation caused strong inhibition of assembly of MIIB$^{\alpha F47}$ and only slight inhibition of that of MIIB$^{\beta F47}$. These results suggest that myosin assembly can be regulated through phosphorylation within the nonhelical domain at the COOH terminus of the heavy chains and that the effects are isoform specific.

Localization of the PK C sites in MIIB$^{\beta F47}$ revealed that Ser-362 and Ser-370 were the favored PK C sites among the cluster of Ser residues in the sequence $^{362}S_{PO_4}$-I-S-F-S-S_{PO_4}-S_{PO_4}-R-$^{370}S_{PO_4}$-. Although PK C is known to phosphorylate Ser/Thr within a basic environment, acidification of the peptide region by phosphorylation at either Ser-362 or Ser-370 did not seem to influence phosphorylation at the other site. However, when Ser-362 was phosphorylated, phosphorylation at the neighboring sites (Ser-364 and Ser-366) seemed to be completely inhibited. This might also be true for the phosphorylation of Ser-367, -368, and -370, i.e., that phosphorylation at Ser-370 inhibits phosphorylation at neighboring sites. If there were no sites that PK C prefers, a mixture of phosphopeptides containing equal ratios of phosphate at various sites would be expected. In the case of MIIB$^{\alpha F47}$, within the peptide region ^{362}P-I-S_{PO_4}-F-S_{PO_4}-S_{PO_4}-S_{PO_4}-R-$^{370}S_{PO_4}$-, PK C seemed to phosphorylate mainly at two sites, Ser-368 and Ser-370, based upon the recovery rates of the peptides and those of free ^{32}P phosphate; Frac-15$_{Therm}$ was more likely a mixture of peptides phosphorylated mainly at Ser-368 or Ser-370 (Figure 12A, Tables 2 and 3). These results suggest that also in MIIB$^{\alpha F47}$ phosphorylation at any one of these five sites results in inhibition of additional phosphorylation within this sequence. However, we do not know the relationship between phosphorylation at Ser-352 (region I, see Figure 13) and the cluster of serine residues (region II).

We found five and four CK II sites in each heavy chain of MIIB$^{\alpha F47}$ and MIIB$^{\beta F47}$, respectively. Because the sequence of human MIIB is identical with that of rabbit MIIB$^{\alpha}$ over the entire nonhelical domain (except for a Leu ↔ Ile replacement at residue 377), we predict that CK II would phosphorylate human MIIB at the sites identified for MIIB$^{\alpha F47}$. The CK II site in native myosin purified from bovine brain was identified previously (*23*) (see Figures 1 and 13). In that study, we detected only one Ser residue as the CK II site. It should be noted that the Thr residue identified in this study as the CK II site in both rabbit MIIB isoforms is replaced with Asp in bovine MIIB (*23*) while chicken MIIB has Ala at this position (*10*) (see Figure 1). However, the next two Ser residues in the sequence, identified as CK II sites in this study, might also be phosphorylatable by CK II in bovine brain myosin since the neighboring amino acid sequences are very similar to those of rabbit MIIBs. There are at least three possibilities why we did not see phosphorylation by CK II at multiple sites in bovine brain myosin: (1) sensitivity of methods used for detection of phosphorylation sites, (2) reduction of the phosphorylation efficiency for native myosins during the long

purification periods, and (3) only one major phosphorylatable site in the bovine brain myosin heavy chain. Regarding the first possibility, the method we used here (*33*) significantly enhanced the sensitivity for identification of the phosphorylation sites. In this method, phosphopeptides were cross-linked to membranes through their COOH groups, preventing the peptides, especially hydrophilic peptides as phosphopeptides usually are, from being washed off the membranes during the Edman degradation reaction cycles. In addition, the manual Edman degradation procedure used here gave excellent repetitive yields and there was no tailing (or carry over) of free phosphate from cycle to cycle (see Figures 9 and 12); these results contrast with those normally seen with a Beckman spinning cup sequencer (890 M liquid-phase sequencer), in which there is always substantial carryover (*23*). This method permitted us to successfully identify the CK II and PK C sites within clusters of phosphorylation sites, using as little as 3000 cpm/peptide as starting material. The method used here is much more sensitive than the one that involves conversion of phosphoserine to S-ethylcysteine by β-elimination and detection of PTH−S-ethylcysteine (*39*). Regarding the second possibility, we found that the phosphorylation efficiencies of heavy chain fragments by both kinases decreased significantly during storage on ice. Because of this, we stored heavy chain fragments in 6 M urea at −70 °C and dialyzed them first against buffers containing 0.6 M salt and then against low salt, overnight, just before use. The proteins were then used within 3−4 days. In the case of myosin isolated from bovine brain, purification requires about 1 week, and additional days are required for dephosphorylation. Therefore, it is possible that during preparation certain levels of denaturation occur within the nonhelical tail domain, which in turn reduces accessibility of some of the CK II sites. However, this does not exclude the third possibility. We have seen differences in the rates of CK II phosphorylation of MIIB$^{\alpha F47}$ and MIIB$^{\beta F47}$ prepared simultaneously and assayed under the same conditions, although these isoforms are quite similar in their amino acid sequences. Bovine brain myosin lacks the phosphorylatable Thr residue within the cluster of acidic amino acids found in rabbit MIIBs (at position 389) because it is replaced by Asp, and the amino acid at position 381 is not known (see Figure 13). So, it is possible that CK II phosphorylates at one major site in the case of bovine brain myosin. In this regard, it would be very interesting to see whether human SM_1 can be phosphorylated by CK II at the Thr and Ser residues that correspond to Thr-389 and Ser-404 in rabbit MIIBs (Figure 1). The CK II sites in SM_1 from bovine (*24*) and porcine (*40*) aortas were identified at the equivalent position to that seen in bovine brain myosin.

PKC-mediated phosphorylation at only one site per heavy chain affected assembly of MIIBs. The PK C site is close to the junction between the α-helical coiled-coil structure and the nonhelical domain. Addition of strong negative charges due to phosphate groups within the highly basic environment near this junction (see Figure 13) may generate a conformational change within this or a nearby region that is sufficient to block filament assembly. Alternatively, the incorporated phosphate group(s) may disturb electrostatic interactions between or among MIIB fragments. It is likely that the effect of PK C phosphorylation of Ser-352 on filament assembly is minor, since PK C phosphorylation at the corresponding site in MIIA^{F46} (E-V-S-S_{PO_4}-L-K-) does not affect assembly (Figure 6); also the levels of phosphorylation at Ser-352 appeared to be much lower than at other PK C sites, for both MIIB isoforms. In contrast, the CK II-mediated phosphorylation seems to inhibit filament assembly only when multiple sites are phosphorylated. The MIIB$^{\beta F47}$ phosphorylated to the extent of 2 mol/mol heavy chain showed only slight inhibition of assembly (Figure 6). In addition, phosphorylation of MIIA^{F46} by CK II at 1 mol/mol peptide at one Ser within the nonhelical tail domain showed no detectable effect on the assembly. (Under these conditions, MIIA^{F46} was also substoichiometrically phosphorylated, at a Thr residue near the end of the α-helical region, T-E-T(PO_4)-A-D-.) Since CK II phosphorylates Ser/Thr within an acidic environment, addition of one phosphate group into such an acidic region may not cause a significant change in its structure. Incorporation of multiple phosphate groups into the acidic amino acid region may be necessary before significant structural changes are seen. Phosphorylation of *Dictyostelium* myosin II in a region about 34 kDa from the COOH terminus blocks myosin assembly (*41*, *42*), apparently by stabilizing a bend in the molecule near the phosphorylation site (*43*). It is unlikely that vertebrate nonmuscle myosin (and possibly smooth muscle myosin) assembly is inhibited by this mechanism because their phosphorylation sites are much closer to the COOH terminus (maximally 55 amino acids from the carboxyl end).

Nonmuscle myosins MIIA and MIIB often distribute within cells in an isoform-specific manner (*5*−*8*). Since both MIIA and MIIB probably have the same or very similar regulatory light chains (*44*, *45*), it seems unlikely to us that phosphorylation of the regulatory light chains can be the mechanism for establishing and maintaining isoform-specific cellular distributions of myosins. In the present study, we have shown that fragments of the heavy chains of three different nonmuscle myosin isoforms exhibit different assembly properties in the presence of various salt concentrations and that the effects of phosphorylation on assembly are isoform specific. Our results suggest that PK C phosphorylates brain myosin heavy chain at serine residue(s) within the tail region. On the basis of the conservation of amino acid sequences among all MIIB isoforms across species lines, we predict that the major PK C site(s) in bovine brain myosin would also lie near the junction between helical and nonhelical domains. Heavy chains of nonmuscle myosin II bind to acidic phospholipids, and this binding is a prerequisite for phosphorylation of heavy chains by PK C within the tail end domain (*27*). Binding of the MIIB$^{\beta F47}$ to membranous PS was also required for its efficient phosphorylation. In conclusion, we propose that the isoform-specific phosphorylation of the heavy chains coordinated with phosphorylation of the light chains, by various combinations of kinases, is a major factor in the regulation of isoform specific myosin assembly in vivo.

ACKNOWLEDGMENT

We thank Sharon Mathier for computer graphics.

SUPPORTING INFORMATION AVAILABLE

Six tables of the detailed results of amino acid analysis and amino acid sequencing and three figures of the results

of manual Edman degradation of the isolated phosphopeptides (9 pp) are included. Ordering information is given an any current masthead page.

REFERENCES

1. Yumura, S., and Fukui, Y. (1985) *Nature 314*, 194−196.
2. Saez, C. G., Myers, J. C., Shows, T. B., and Leinwand, L. A. (1990) *Proc. Natl. Acad. Sci. U.S.A. 87*, 1164−1168.
3. Simons, M., Wang, M., McBride, O. W., Kawamoto, S., Yamakawa, K., Gdula, D., Adelstein, R. S., and Weir, L. (1991) *Circ. Res. 69*, 530−539.
4. Toothaker, L. E., Gonzalez, D. A., Tung, N. R., Lemons, S., LeBeau, M. M., Arnaout, M. A., Clayton, L. K., and Tenen, D. G. (1991) *Blood 78*, 1826−1833.
5. Borrione, A. C., Zanellato, A. M. C., Giuriato, L., Scannapieco, G., Pauletto, P., and Sartore, S. (1990) *Exp. Cell Res. 190*, 1−10.
6. Cheng, T. P. O., Murakami, N., and Elzinga, M (1992) *FEBS Lett. 311*, 91−94.
7. Maupin, P., Phillips, C. L., Adelstein, R. S., and Pollard, T. D. (1994) *J. Cell Sci. 107*, 3077−3090.
8. Kelley, C. A., Sellers, J. R., Gard, D. L., Bui, D., Adelstein, R. S., and Baines, I. C. (1996) *J. Cell Biol. 134*, 675−687.
9. Shohet, R. V., Conti, M. A., Kawamoto, S., Preston, Y. A., Brill, D. A., and Adelstein, R. S. (1989) *Proc. Natl. Acad. Sci. U.S.A. 86*, 7726−7730.
10. Takahashi, M., Kawamoto, S., and Adelstein, R. S. (1992) *J. Biol. Chem. 267*, 17864−17871.
11. Kuro-o, M., Nagai, R., Nakahara, K., Katoh, H., Tsai, R.-C., Tsuchimoto, H., Yasaki, Y., Ohkubo, A., and Takaku, F. (1991) *J. Biol. Chem. 266*, 3768−3773.
12. Phillips, C. L., Yamakawa, K., and Adelstein, R. S. (1995) *J. Muscle Res. Cell Motil. 16*, 379−389.
13. Babij, P., and Periasamy, M. (1989) *J. Mol. Biol. 210*, 673−679.
14. Nagai, R., Kuro-o, M., Babij, P., and Periasamy, M. (1989) *J. Biol. Chem. 264*, 9734−9737.
15. Yanagisawa, M., Hamada, Y., Katsuragawa, Y., Imamura, M., Mikawa, T., and Masaki, T. (1987) *J. Mol. Biol. 198*, 143−157.
16. Matsuoka, R., Yoshida, M. C., Furutani, Y., Imamura, S., Kanda, N., Yanagisawa, M., Masaki, T., and Takao, A. (1993) *Am. J. Med. Genet. 46*, 61−67.
17. Tashiro, Y., Kumon, A., Yasuda, S., Murakami, N., and Matsumura, S. (1985) *Eur. J. Biochem. 148*, 521−528.
18. Cross, R. A., and Vanderkerckhove, J. (1986) *FEBS Lett. 200*, 355−360.
19. Maeda, K., Rosch, A., Maeda, Y., Kalbitzer, H. R., and Wittinghofer, A. (1991) *FEBS Lett. 281*, 23−26.
20. Ikebe, M., Hewett, T. E., Martin, A. F., Chen, M., and Hartshone, D. (1991) *J. Biol. Chem. 266*, 7030−7036.
21. Hodge, T. P., Cross, R. A., and Kendrick-Jones, J (1992) *J. Cell Biol. 118*, 1085−1095.
22. Dibb, N. J., Brown, S. L., Karn, J., Moerman, D. G., Bolton, S. L., Waterston, R. H. (1985) *J. Mol. Biol. 205*, 543−551.
23. Murakami, N., Healy-Louie, G., and Elzinga, M. (1990) *J. Biol. Chem. 265*, 1041−1047.
24. Kelley C. A., and Adelstein, R. S. (1990) *J. Biol. Chem. 265*, 17876−17882.
25. Conti, M. A., Sellers, J. R., Adelstein, R. S., and Elzinga, M. (1991) *Biochemistry 30*, 966−970.
26. Murakami, N., Elzinga, M., Singh, S. S., and Chauhan, V. P. S. (1994) *J. Biol Chem. 269*, 16082−16090.
27. Murakami, N., Singh, S. S., Chauhan, V. P. S., and Elzinga, M. (1995) *Biochemistry 34*, 16046−16056.
28. Murakami, N., Matsumura, S., and Kumon, A. (1984) *J. Biochem. 95*, 651−660.
29. Huang, K. P., Nakabayashi, H., and Huang, F. L. (1986) *Proc. Natl. Acad. Sci. U.S.A. 83*, 8535−8539.
30. Hannun, Y. A., Loomis, C. R., and Bell, R. M. (1985) *J. Biol. Chem. 260*, 10039−10043.
31. Lowry, O. H., Rosebrough, N. J., Farr, A. L., and Randall, R. J. (1951) *J. Biol. Chem. 193*, 265−275.
32. Muszynska, G., Anderson, L., and Porath, J. (1986) *Biochemistry 25*, 6850−6853.
33. Sullivan, S., and Wong, T. W. (1991) *Anal. Biochem. 197*, 65−68.
34. Hunter, T., and Sefton, B. M. (1980) *Proc. Natl. Acad. Sci. U.S.A. 77*, 1313−1315.
35. Hathaway, G. M., and Trough, J. A. (1982) *Curr. Top. Cell Regul. 21*, 101−127.
36. Ikeda, N., Yasuda, S., Muguruma, M., and Matsumura, S. (1990) *Biochem. Biophys. Res. Commun. 169*, 1191−1197.
37. Matsumura, S., Kumon, A., and Chiba, T. (1985) *J. Biol. Chem. 260*, 1959−1966.
38. McLachlan, A. D., and J. Karn (1982) *Nature 299*, 226−231.
39. Meyer, H. E., Hoffman-Poroska, E., Korte, H., and Heilmeyer, L. M. (1986) *FEBS Lett. 204*, 61−66.
40. Fukui, Y., and Morita, F. (1996) *J. Biochem. 119*, 783−790.
41. Vaillancourt, J. P., Lyons, C., Côte, G. P., (1988) *J. Biol. Chem. 263*, 10082−10087.
42. Lück-Vielmetter, D., Schleicher, M., Grabatin, B., Wipper, J., and Gerisch, G. (1990) *FEBS. Lett. 269*, 239−243.
43. Pasternak, C., Flicker, P. F., Ravid, S., and Spudich, J. A. (1989) *J. Cell Biol. 109*, 203−210.
44. Taubman, M. B., Grant, J. W., and Nadal-Ginard, B. (1987) *J. Cell Biol. 104*, 1505−1513.
45. Feinstein, D. L., Durand, M., and Milner, R. J. (1991) *Mole. Brain Res. 10*, 97−105.

BI971959A